University of Southern Queensland

Faculty of Engineering and Surveying

AN EXPERIMENTAL AND THEORETICAL INVESTIGATION OF SIDE WEIRS

A dissertation submitted by

David Selwyn Rowlings

in fulfilment of the requirements of

Courses ENG4111 and 4112 Research Project

towards the degree of

Bachelor of Engineering (Civil)

Submitted: October, 2010

Abstract

The aim of this research is to determine the validity of available theoretical approaches for the side weir problem. This will be done with the experimental results gained from experimentation conducted in the hydraulics lab. It is hoped that the project will result in a more general solution for side weir problems that allows designers a greater amount of flexibility in weir configurations.

This dissertation has examined methods of solution for the side weir problem based on theory found during a literature review. An experimental flume was constructed for the specific purpose of side weir experimentation. Experimental results have been compared with available theory in An attempt to validate the theory available, however incomplete and inaccurate data from the experimental work has hindered this process. As time was not permitting no attempt was made to formulate and validate a more complete method of solution

University of Southern Queensland

Faculty of Engineering and Surveying

ENG4111 & ENG4112 *Research Project*

Limitations of Use

The Council of the University of Southern Queensland, its Faculty of Engineering and Surveying, and the staff of the University of Southern Queensland, do not accept any responsibility for the truth, accuracy or completeness of material contained within or associated with this dissertation.

Persons using all or any part of this material do so at their own risk, and not at the risk of the University of Southern Queensland, its faculty of Engineering and Surveying or the staff of the University of Southern Queensland.

This dissertation reports an educational exercise and has no purpose or validity beyond this exercise. The sole purpose of the course pair entitled "Research Project" is to contribute to the overall education within the student's chosen degree program. This document, the associated hardware, software, drawings, and other material set out in the associated appendices should not be used for any other purpose: if they are so used, it is entirely at the risk of the user.

Prof Frank Bullen

Dean

Faculty of Engineering and Surveying

Certification

I certify that the ideas, designs, and experimental work, results, analyses and conclusions set out in this dissertation are entirely my own effort, except where otherwise indicated and acknowledged.

I further certify that the work is original and has not been previously submitted for assessment in any other course or institution, except where specifically stated.

David Selwyn Rowlings

Student Number: w0071985

_____

Signature

_____

Date

Table of Contents

List of Figures

List of Tables

CHAPTER 1

1. INTRODUCTION

1.1 Overview of the Problem

The side weir problem is one that is vastly more complex than a typical weir situation. It is an arrangement that occurs frequently throughout civil and agricultural engineering fields. Ambiguities are evident in many texts and journals which deal with the side weir problem so an investigation has taken place to clarify and expand knowledge of the topic. The intent of this project is to clarify the available theory on side weirs by comparison with experimental data.

1.2 Significance of the Problem

Side weir flow has been examined in a variety of journals and texts. There has been no definitive method of solving this problem in all of the research conducted. As side weirs are used extensively throughout irrigation channels, as storm water overflows and in other civil infrastructure, accurate and reliable design methods are important.

It is important to note that there are several empirical methods of solution which are reliable and produce reasonably accurate results. As with many empirical methods though, the range in which the method is useful is limited. This limitation means that when a design is required for a situation which occurs outside of the empirical methods accurate range that more in-depth experimentation or analysis is required.

For this reason it is important to have a solution method which is both accurate and robust. It is this which is the critical aspect of the side weir problem, as finding a solution method which is both of these will allow for effective and efficient practice in the design and use of side weirs. To date no complete and proven analytical solution is available, which is largely due to the large number of parameters which need to be considered in such a problem.

1.3 Background Information on Side Weirs

A side weir is a lateral outflow structure which is located in the side of a channel, as opposed to straight across the channel. As a weir its' purpose is a control and measurement point. Typically weirs are classified as a flow measuring structure (*Chadwick et al, 2004*) however it is important to note that the side weir also acts as a discharge structure in the same way the spillway does.

Side weir flow can be described in terms of a change in momentum or a change in energy, and this thesis will examine in part the accuracy of one over the other. It is thought that the principles of momentum will provide the more accurate results as it is more suitable for this particular case as. This is because no *energy losses* are seen over the weir, just a momentum change as a portion of the water ejects from the side weir.

Side weirs have been researched extensively and finding relevant literature is not a hard task. On the other hand, finding literature which sets out a means of solution in a clear and precise manner is not so easy to come by. Many of the solutions found are empirical, and do not cover a wide range of side weir applications or situations.

Ramamurthy and Carballada (*1980*) propose a method of solution which is based on the free efflux theory of McNown and Hsu (*1954).* This solution examines the geometric configurations and the velocity ratios to find a total discharge. The method uses a taylor series approximation a coefficient of discharge which can be used to calculate the weir discharge.

Hager (*1987*) examined the diminishing velocity over the length of the weir. This decrease in lateral outflow intensity is demonstrated in Figure 1.1, which is a summary of Hager's experiments, and clearly shows that the discharge angle is decreasing over the weir length.

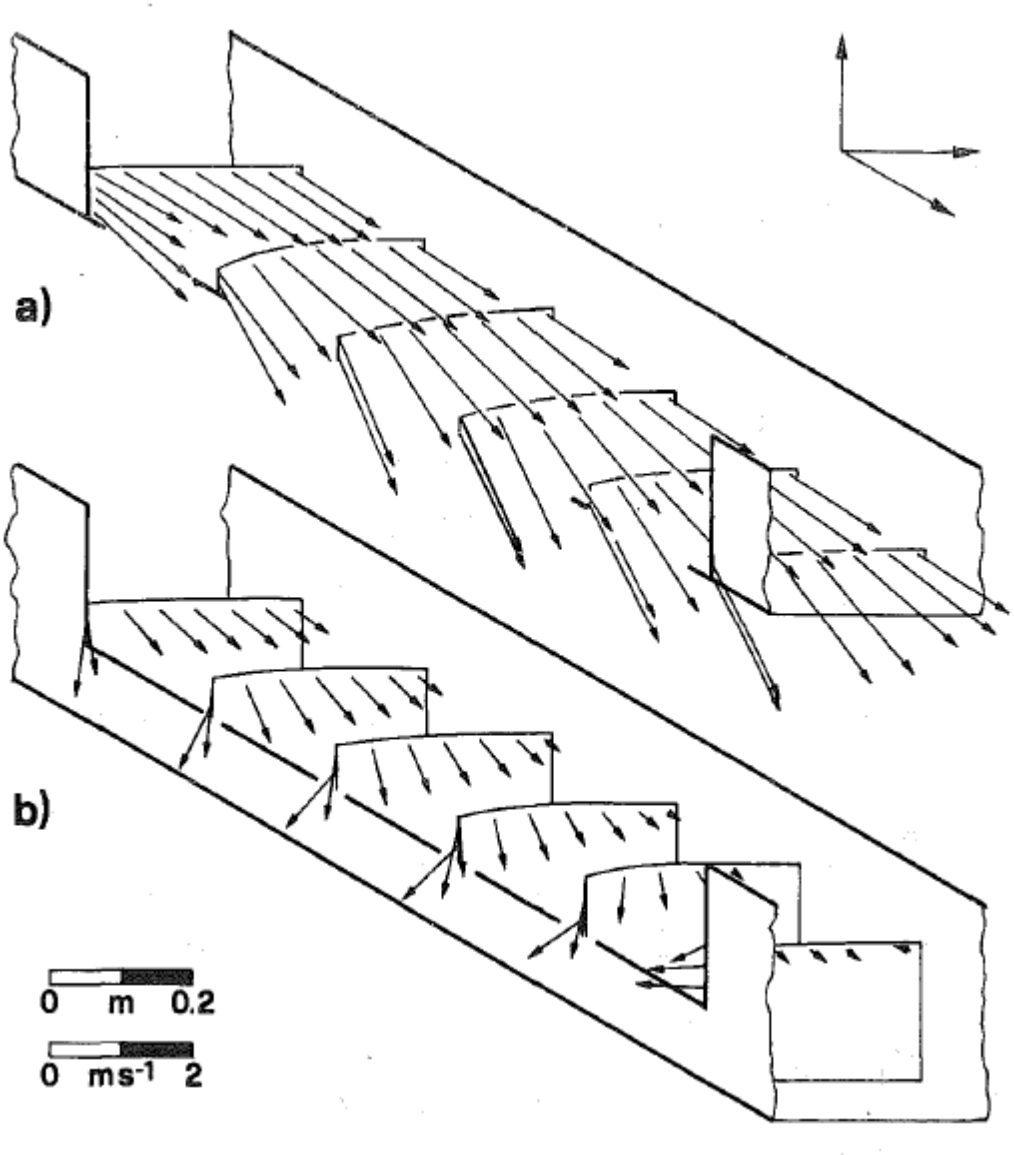

Figure 1-1 Lateral Outflow and Surface Velocity Profiles (sourced: Hager, *1987*)

Muslu (*2001*) conducted a numerical analysis of side weirs which examined them by using a variation of De Marchi's (*1934)* integral solution method. This slight alteration takes the stance that the weir coefficient and discharge angle are not in fact constant, as De Marchi assumed, but functions of several parameters. Doing this complicated the problem to such an extent that it could only be solved using an iterative process.

Muslu (*2001*) also compiled a comparison of several empirical methods and their results. This comparison shows the wide variation that occurs in solutions of side weir problems. The range of the geometric configurations and the corresponding weir discharge coefficient vary considerably across the different methods given the same Froude number, upstream depth and height of the weir.

One method which clearly outlines a solution and is based on the gradually varied flow principles is that presented by Chow (*1959*) in the text *Open Channel Hydraulics.* This theory outlines a method for lateral inflow and outflow; however derivation of the two cases is different. It is the difference in derivation of these equations which gives rise to ambiguities and makes the accuracy of this method questionable.

Prior to this thesis it appears that no work has been carried out examining the change in parameters between discrete and long weirs. Using the discrete weir will hopefully give insights into the changing angle of discharge and discharge coefficient.

1.4 Project Objectives

The crux of this project is a comparison between theoretical and experimental analysis of side weirs. In doing this it is hoped a better understanding of the available theory will be reached. The essential element to allowing this to happen will be the comparison between the discrete side weir and the weir the same width as the main channel. This should provide insights into the geometric and velocity ratios.

The experimental process aims to characterise the side weir problem by examining different weir lengths. Using vastly different weir lengths under the similar flow conditions will allow the robustness of currently solution methods to be tested. It will also show how the side weir characteristics differ with the length of the weir.

1.5 Scope of Thesis

This thesis has a large scope, as it attempts to validate current theory by comparison with experimental results. It is also looking at whether anything can be learned by examining the discrete lateral slot, in comparison with the longer weir. The project therefore includes a large variety of techniques, including:

- Experimentation
- Computer modeling of experimental results
- Empirical analysis
- Numerical analysis
- Analytical analysis
- Comparative analysis of all modeling and results

CHAPTER 2

2. BACKGROUND THEORY

2.1 Theory and Modelling

The ability to derive relevant theories and in some cases laws of nature for a physical situation, allows us to make predictions, and model these circumstances. This is the essence of most engineering fields and as such it is very important, in particular to this thesis.

Several laws and theories are very important to the side weir problem and these will be presented systematically in this chapter. It is important to note that some of these are only theories, and as such their accuracy, in some circumstances, is not always guaranteed; however all of what is presented here is used widely within engineering practice.

2.2 Fundamental Laws of Fluid Dynamics

2.2.1 Conservation of Mass

The law of conservation of matter states that *'matter can be neither created nor destroyed, though it may be transformed (e.g through chemical process)'*. As fluid dynamics in civil applications does not involve any chemical transformations this can be simplified to the conservation of mass. This means that the mass entering a control volume will equal the mass leaving the control volume, and is represented in its simplest form by equation 2-1. Conservation of mass is used in the solution of all fluid dynamic problems (*Chadwick et al., 2004*).

$$Q = VA \qquad \text{Eq 2-1}$$

2.2.2 Conservation of Energy

The law of conservation of energy states that '*energy may neither be created nor destroyed'*. It can be transformed from one form to another, such as potential to kinetic, but it cannot be destroyed. The term energy loss is sometimes used, however this just refers to the energy being lost from the water and being transferred to heat for example with friction losses (*Chadwick et al, 2004*). In hydraulic problems the energy equation is most regularly used in the form of the Bernoulli equation; equation 2-2 below. Equation 2-2 can be broken down into segments of *Pressure Head, Kinetic Head* and *Potential Head.*

$$\frac{P_1}{\rho_1 g} + \frac{u_1}{2g} + z_1 = \frac{P_2}{\rho_2 g} + \frac{u_2}{2g} + z_2 = H = constant \qquad \text{Eq 2-2}$$

Currently most side weir solution methods employ the use of this theory. It is this which is a point of contention as the momentum law seems more applicable.

2.2.3 Conservation of Momentum

The law of conservation of momentum states that '*a body in motion cannot gain or lose momentum unless some external force is applied'*. This is Newton's second law of motion, and as such has applications to fluid dynamics. The simplest form of this equation is momentum entering equals momentum leaving, which is demonstrated in equation 2-3.

$$\rho\delta Q_1\delta tu_1 = \rho\delta Q_2\delta tu_2 \qquad \text{Eq 2-3}$$

This equation however cannot be applied in this form to the side weir problem as the flow is being divided at the downstream end of the control volume. Therefore the equation used will be of the form of equation 2-4, with first term being the flow upstream of the weir, the second term the flow immediately downstream of the weir and the third term representing the portion of flow going over the side weir.

$$\rho\delta Q_1\delta tu_1 = \rho\delta Q_2\delta tu_2 + \rho\delta Q_3\delta tu_3 \qquad \text{Eq 2-4}$$

2.3 Laminar and Turbulent Flow

It is important to differentiate between the types of flow which are occurring within a channel. In open channel problems the type of flow will determine how accurately the problem can be solved.

Laminar flow is when the flow is seen to be flowing in straight streamlines which do not mix with one another. Turbulent flow on the other hand is where the streamlines are mixed and irregular, with the possibility of eddies forming, depending on how turbulent the water is. In between the two types is a transitional zone where the water is neither here nor there, with partial turbulence and partial laminar flow (*Chadwick et al., 2004*). The three types of flow are depicted in figure 1 below.

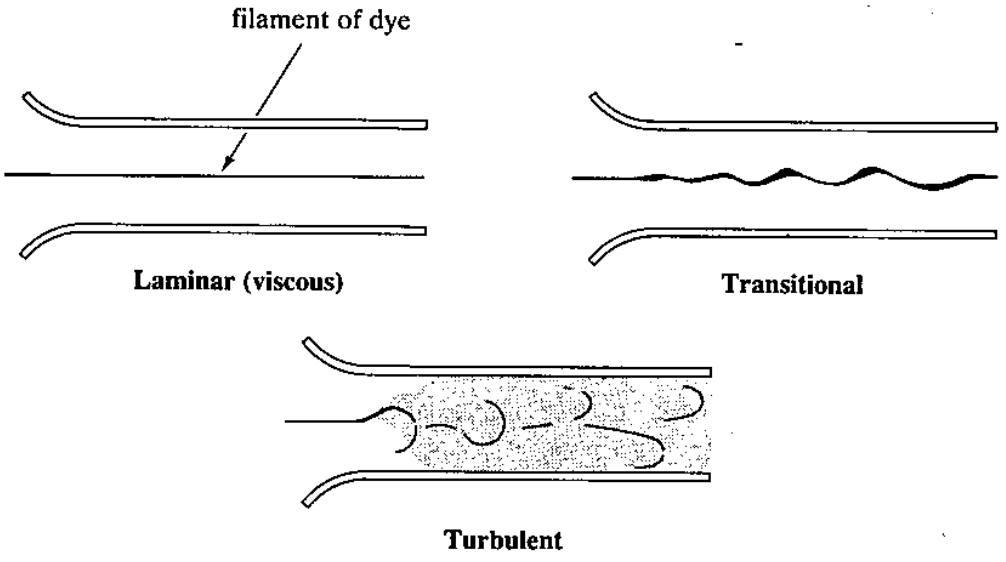

Figure 2-1 - Laminar, Transitional and Turbulent Flow

Source: Chadwick et al. (2004, p70)

These flows can be classified depending on the value of the Reynolds number. For open channel flow a value of 500 or less implies laminar flow, 1000 or greater turbulent, and between the two is the transition zone (*Chadwick et al., 2004*). Reynolds number for open channel flow can be calculated using equation 2-5.

$$Re = \frac{\rho RV}{\mu} \qquad \text{Eq 2-5}$$

2.4 Froude Number

For open channel flow the Froude number defines the regime of flow (*Chadwick et al., 2004*). It is useful as the momentum and energy equations can be written in terms of the Froude number (*Chadwick et al., 2004*). The flow regimes are as follows:

Fr < 1 *Subcritical* flow; relatively deep, slow flow

Fr = 1 *Critical* flow; transitional flow

Fr > 1 *Supercritical* flow; relatively shallow, fast flow

These flow regimes can be defined in terms of waves, equation 2-6, subcritical flow will allow a wave to propagate upstream. Supercritical on the other hand will not allow a wave to propagate upstream. The critical flow condition is the boundary condition where the velocity of the wave trying to propagate is exactly equal to the velocity in the channel (ie. Velocity is equal to $\sqrt{gy}$).

$$Fr = \frac{water\ velocity}{wave\ velocity} = \frac{V}{\sqrt{gy}} \qquad \text{Eq 2-6}$$

2.5 Darcy-Weiscbach and Colebrook-White Equations

The Darcy-Weisbach equation (2-7) as used in pipe problems can be modified for the open channel situation by the substitution of equations 2-8 and 2-9 to give the equation 2-10 (*Chadwick et al., 2004*). Equations 2-8 and 2-9 convert pipe figures into forms which can be used for open channel purposes.

$$h_f = \frac{fLV^2}{2gD} \qquad \text{Eq 2-7}$$

$$R = \frac{D}{4} \qquad \text{Eq 2-8}$$

$$S_0 = \frac{h_f}{L} \qquad \text{Eq 2-9}$$

$$f = \frac{8gRS_o}{V^2} \qquad \text{Eq 2-10}$$

If the Colebrook-White equation (2-11) has the open channel variation of the Darcy-Weisbach equation substituted into it, equation 2-12 is formulated, and then a solution is possible for mean section velocity, *V*.

$$\frac{1}{\sqrt{f}} = -2\log\left(\frac{k}{14.8R} + \frac{2.51\nu}{4RV\sqrt{f}}\right) \qquad \text{Eq 2-11}$$

$$V = -\sqrt{32gRS_o}\log\left(\frac{k}{14.8R} + \frac{1.255\nu}{R\sqrt{32gRS_o}}\right) \qquad \text{Eq 2-12}$$

This equation is used when flow is not rough turbulent, as the Manning equation is not very accurate in the other zones. It is when friction is very low that a small difference in manning's *n* cause big variations in velocity.

The accuracy of the Darcy-Weisbach, Colebrook-White method is also questionable as the formulae are derived from equations for pressurised pipe flow where the frictional resistance is uniformly distributed (*Chadwick et al., 2004*). In the open channel case, because of the free surface, the velocity distribution is affected because the frictional resistance is non-uniformly distributed around the boundary (*Chadwick et al., 2004*). Even considering this, it is still a more reliable method of solution in the laminar and transitional zones, even if not completely accurate.

2.6 Manning's Equation

The manning equation is one of most widely used equations for open channel flow characteristics. Given the bed slope, hydraulic radius and Manning's n value, the mean section velocity of the channel can be easily computed. This equation has the benefit of being simple and accurate, when within the rough turbulent zone (*Chadwick et al, 2004*).

Manning derived this equation from the Chezy equation (2-13) and that the Chezy coefficient, *C*, could be replaced by $R^{1/6}/n$ (*Nalluri et al., 2001)*. This resulted in the Manning equation as can be seen in equation 2-14.

$$V = C\sqrt{RS_o} \qquad \text{Eq 2-13}$$

$$V = \frac{1}{n} R^{2/3} S_o{}^{1/2} \qquad \text{Eq 2-14}$$

This equation is an empirical one however it is a very effective one which makes solution of these problems a lot simpler than they would otherwise be. The manning *n* value is assigned according to the surface condition of the channel. These values were calculated based on experimental data from Bazin (*Chow, 1959*).

As Manning's equation is simple to use it has become standard practice to solve open channel problems with it.

2.7 Gradually Varied Flow

This is a type of flow which is defined as being steady and non uniform, typified by a smooth back water profile. The side weir case is an example of a gradually varied flow situation when subcritical flow conditions exist upstream of the weir. Gradually varied flow is where the discharge passing through the channel cross sections is a constant, but the depth, width and mean velocity may change gradually between the sections (*Hamill, 2001*).

There are three forms of the gradually varied flow equation however the one of most interest in this case is equation 2-15 below. This equation can be reworked to give equation 2-16, so that it acts as a finite difference solution, where with each step of x a change in height is returned (*Chadwick et al., 2004*). This method is known as the direct step method and is used to solve many gradually varied flow problems.

$$\frac{dy}{dx} = \frac{S_o - S_f}{1 - Fr^2} \qquad \text{Eq 2-15}$$

$$\Delta y = \Delta x \left(\frac{S_o - S_f}{1 - Fr^2}\right) \qquad \text{Eq 2-16}$$

2.8 Contracted Weir Discharge

The weir equation is very similar to the orifice equation and it has been proposed that a weir can be thought of as a large orifice where the water surface has fallen below the top of the opening (*Hamill, 2001*).

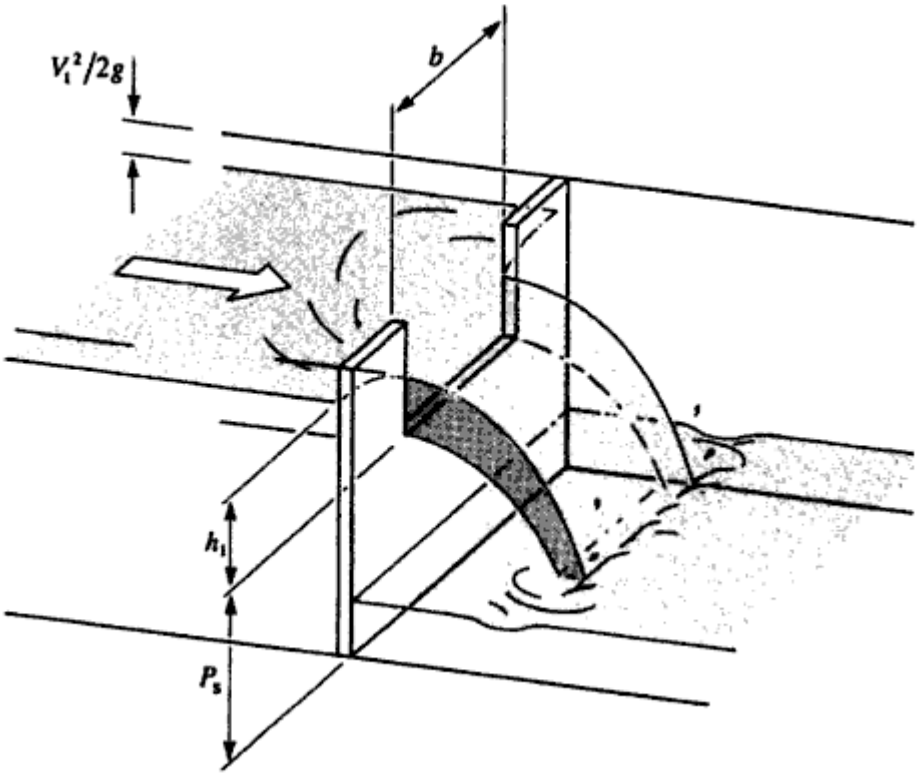

Figure 2 -2 - Contracted Weir

Source: Chadwick et al. (2004, p432)

Contracted weirs are characterised by the contraction of the sides of the flow as it springs clear of the weir. This contraction means the discharge calculation will vary from that of a full-width weir (*Chadwick et al., 2004*). For a full-width weir the discharge is defined by equation 2-17. This equation does not hold true for the contracted weir because it does not account for the changing flow path as the water ejects from the weir.

$$Q_t = \frac{2}{3} b \sqrt{2g} {h_1}^{2/3} \quad \text{Eq 2-17}$$

To account for the contraction of the flow after it expels from the weir a coefficient of discharge has been formulated to allow for this phenomena. This coefficient can be calculated by a couple of means, either with the Hamilton-Smith equation (equation 2-18), or by using experimental discharges as *Q* in equation 2-19 (*Chadwick et al., 2004*).

$$C_d = 0.616 \left(1 - \frac{h_1}{P_s}\right) \quad \text{Eq 2-18}$$

$$C_d = \frac{Q}{Q_{ideal}} \quad \text{Eq 2-19}$$

Equation 2-18 can be used in conjunction with equation 2-17 to calculate the actual discharge of the weir; combining the two yields equation 2-20.

$$Q_t = \frac{2}{3} C_d b \sqrt{2g} {h_1}^{2/3} \quad \text{Eq 2-20}$$

Using equation 2-20 will allow the accurate calculation of weir discharge. It is important to note this is equation is important to this thesis as a comparison to the side weir equations that have been developed by others.

CHAPTER 3

3. METHODOLOGY

3.1 Theoretical Considerations

3.1.1 Angle of Discharge

The importance of the angle of discharge is of particular importance in side weir problems. As the water gets further along the weir the less longitudinal momentum there is pushing it which mean that the discharge angle will increase. This was demonstrated by Hager (1987) with several experiments, this is illustrated in Figure 1.1, which represents the water surface velocity during side weir experimentation. In Figure 1.1 it can be seen that the discharge angle increases with length along the weir. This will be important to keep in mind during the experiments.

3.1.2 Water Surface Profile

Collinge (1957) showed that the water surface profile of the weir will change depending on variances in flow condition and bed slope. It can be seen from Figure 1.2 that under varying flow conditions the water surface profile will change. This is important to

note as the results will need to be required with as little variability in flow conditions as possible.

In figure 1.2 the first case is a critical flow regime upstream of the weir, the second is a subcritical flow regime upstream of the weir and the third is a super critical flow regime upstream of the weir. As a subcritical flow is wanted for the experimental stage, these flow profiles are important to note, as they will give a good assessment of what flow regime is occurring within the channel.

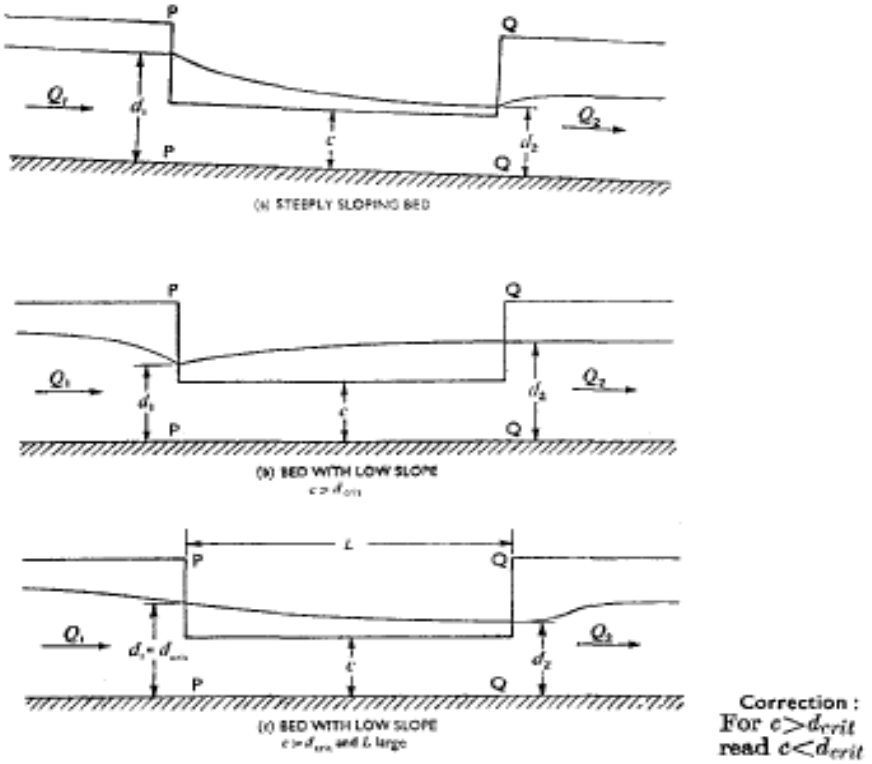

Figure 3-1 – Weir Water Surface Profiles

Source: Collinge, V (1957)

3.2 Theoretical Models

3.2.1 Lateral Flow

Chow (1959) presents a means of solving the side weir problem using analytical techniques in the text Open-Channel Hydraulics. In the text chow divides lateral flow problems into two distinct categories, lateral inflow, where water is added to the main body of flow, and lateral outflow where water is lost from the main body of flow.

In the text Chow (1959) derives the equation for the solution of lateral inflow using the principles of momentum in conjunction with conservation of mass. The equation is derived from Eq 3-1 derivation yields Eq 3-2 as shown below. This can be altered to include the coriolis coefficient, α, in front of the Q terms (as shown in Eq 3-3 below), if a non-uniform velocity distribution is being considered.

$$\rho[QdV + (V + dV)dQ] = -\rho gAdy + \rho gS_oAdx \qquad \text{Eq 3-1}$$

$$\frac{dy}{dx} = \frac{S_o - S_f - 2Qq_*/gA^2}{1 - Q^2/gA^2D} \qquad \text{Eq 3-2}$$

$$\frac{dy}{dx} = \frac{S_o - S_f - 2\alpha Qq_*/gA^2}{1 - \alpha Q^2/gA^2D} \qquad \text{Eq 3-3}$$

For the case of lateral outflow Chow (1959) derives the equation using the energy principle instead of momentum. No reason is stated for this and is justified by the statement that '*the energy principle is directly applicable'*. The derivation yields the expression for lateral outflow shown below in Eq 3-3. This can also be altered for the addition of the coriolis coefficient as in Eq 3-4.

$$\frac{dy}{dx} = \frac{S_o - S_f - Qq_*/gA^2}{1 - Q^2/gA^2D} \quad \text{Eq 3-4}$$

$$\frac{dy}{dx} = \frac{S_o - S_f - \alpha Qq_*/gA^2}{1 - \alpha Q^2/gA^2D} \quad \text{Eq 3-5}$$

It can be seen that there is a difference in the coefficient of the third term of the numerator in Eq 3-2 and Eq 3-4. Chow (1959) explains this difference by saying that '*the momentum principle can also be used to for the derivation of Eq 3-4. In a spatially varied flow, with decreasing discharge, no momentum is added to the water. Following a procedure similar to the derivation of Eq 3-2, the term containing dQ may be dropped from Eq 3-1; the resulting equation will be identical with Eq 3-2'.*

The logic behind this decision to drop the dQ component is questionable. The statement that no momentum is being added to the water is correct; however momentum is being lost from the main body of fluid. This would apply that dQ would change sign, from positive to negative, as this would represent the fact that momentum is being lost in the water ejecting from the side weir.

Another query with this work is why Chow has chosen to derive the inflow equation using momentum principles and the outflow equation using energy principles. The energy equation deals with kinetic, potential and pressure changes. At a junction in a gradually

varied open channel flow problem, like a side weir, there will only be a kinetic energy change to be considered over the control volume; as there will be no significant change in potential and open channel flow experiences no pressure. Such a change is better considered by the momentum equation as it is more capable of handling the altered direction of flow.

It is worth noting the similarities between Chows lateral flow equations and the gradually varied flow formula, equation 2-15. These lateral flow equations can be treated in a similar way to equation 2-15, and a solution is achievable by using the direct step method.

3.2.2 Free Efflux

The theory of free efflux was proposed by McNown and Hsu (1951) which provides a solution for a jet issuing from a lateral slot in a pipe or conduit. This uses a series of conformal transformations to solve the left side of equation 3-6.

$$\oint H_p \, dy = \rho V_j^2 C_c a \sin\theta \qquad \text{Eq 3-6}$$

This led to the formulation of equations 3-7, 3-8 & 3-9.

$$\frac{a}{b} = F\left(\frac{V_1}{V_j}\right) - F\left(\frac{V_2}{V_j}\right) - \frac{V_1 - V_2}{V_j} G(\alpha) \qquad \text{Eq 3-7}$$

Where:

$$F\left(V/V_j\right) = (2/\pi)\left(1 + V^2/V_j^2\right) \tanh^{-1} V/V_j \qquad \text{Eq 3-8}$$

With the expression for $F\left(V_c/V_j\right)$being in the same form

$$G(\theta) = (2/\pi) \cos\theta . \ln\left(\cot\frac{\theta}{2}\right) - \sin\theta \qquad \text{Eq 3-9}$$

Smith (1988) presented a correction for these equations with the inclusion of the energy coefficient α. The equations have been presented as a graphical summary which is shown in figure 3.1.

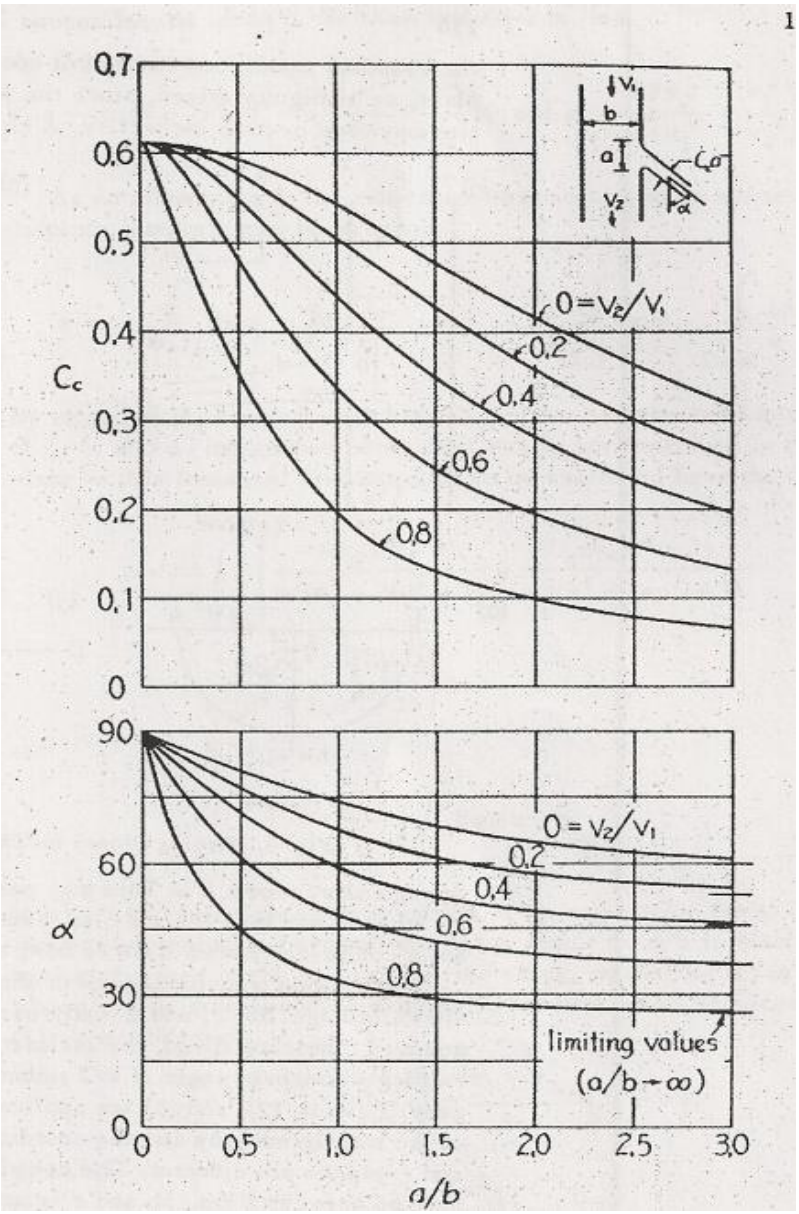

Figure 3-2 – Characteristics of Free Efflux

Source: McNown and Hsu (1951)

McNown and Hsu mention that the work has a potential to act as a guide in experimental work with side weirs. It is possible that this method could become a tool to evaluate or formulate a new method of solving the side weir problem.

3.2.3 Lateral Weir Flow Model

Ramamurthy and Carballada (1980) proposed a method of solving side weir problems. This empirical solution has used techniques described in McNown and Hsu (1951) theory of free efflux.

This model uses the velocity ratio, which is velocity upstream of the weir divided by the velocity of the water ejecting from the weir (Eq 3-10), and the geometric ratio, which is the length of the weir divided by the channel width, to define a coefficient of discharge for the side weir. Unlike many other models it does not attempt to account for the angle of discharge, instead allowing these other two parameters to be the defining factors.

$$\eta = \frac{V_1}{V_j} \qquad \text{Eq 3-10}$$

The equation for the side weir coefficient of discharge is a Taylor series approximation, Eq 3-11. It has numerous variables and is as such more readily solved using the taylor series; however this limits its use to certain situations, namely:

- The bed of the channel is horizontal
- The flow in the channel upstream of the weir is subcritical
- The length of the weir is limited to the width of the parent channel
- The normal velocity component of Vj through any layer is equal to $\sqrt{2gh}$, where h is the depth of the layer below the free surface

$$Q_t = \overline{C_d} L h_o \left\{ V_1 \frac{{F_o}^2}{3} \left[\left(1 + \frac{2}{F_o} \right)^{3/2} - 1 \right] \right\} \qquad \text{Eq 3-11}$$

Where:

$$\overline{C_d} = \frac{3f\left(\eta_o, \frac{L}{B}\right)}{\left(1+\frac{2}{{F_o}^2}\right)^{3/2}-1} \quad \text{Eq 3-12}$$

$$f\left(\eta_o, \frac{L}{B}\right) = (1-{\eta_o}^3)\left(\frac{c_3}{3}+\frac{0.203}{{\eta_o}^3}\right)+(1-\eta_o)\left(c_2+\frac{c_1}{\eta_o}\right) \quad \text{Eq 3-13}$$

$$c_1 = -0.54 + 0.25\left(\frac{L}{B}\right) \quad \text{Eq 3-14}$$

$$c_2 = 0.058 + 0.234\left(\frac{L}{B}\right) \quad \text{Eq 3-15}$$

$$c_3 = -0.13 + 0.49\left(\frac{L}{B}\right) \quad \text{Eq 3-16}$$

$$F_o = \frac{F_1}{\sqrt{Sy_1}} \quad \text{Eq 3-17}$$

$$F_1 = \frac{V_1}{\sqrt{2gy_1}} \quad \text{Eq 3-18}$$

$$\eta_0 = \frac{1}{\left(1+\frac{2}{{F_o}^2}\right)^{1/2}} \quad \text{Eq 3-19}$$

$$h_o = y_1 - S \quad \text{Eq 3-20}$$

In the above equations the channel width (B), weir width (L), upstream velocity (V_1), height of weir (S) and upstream water height (y_1) are all known. This allows a relatively simple solution by substituting these known values into the equations.

It is worth noting that this method does not include direct use of the angle of discharge over the weir. This is accounted for by using the velocity of the water over the weir (V_j) in direct proportion to the upstream velocity (V_1). This still only accounts for the discharge as a single entity that does not change with progression along the weir.

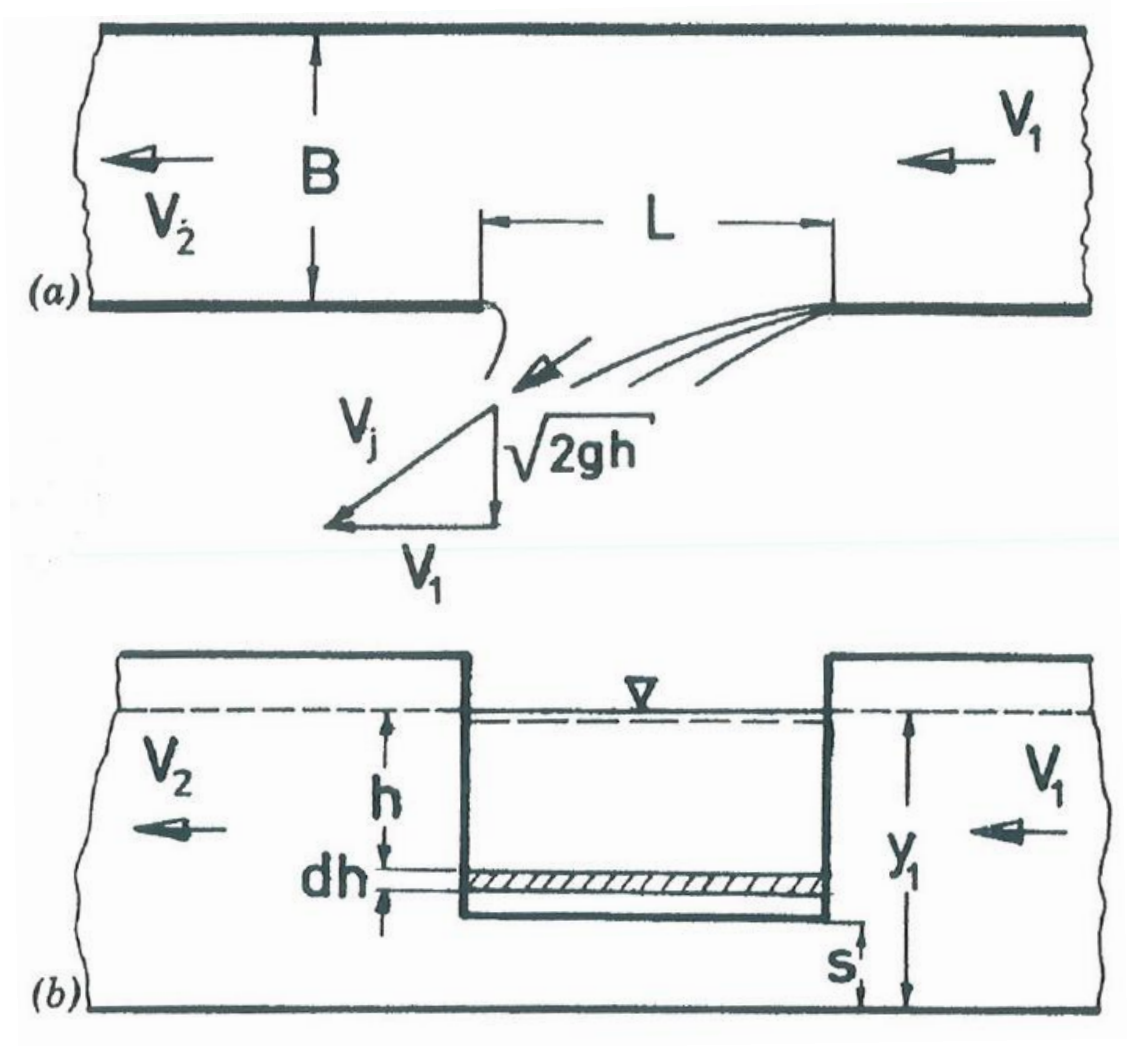

Figure 3-3 – Lateral Flow Model

3.2.4 Numerical Analysis

Muslu (*2001*) model has made mention of the fact that the angle of discharge and the water height across the channel are not a constant across the length of the weir. It also notes that these characteristics are liable to change for different geometric configurations of the weir (*ie. weir length and channel width*). This is very different from most other theories which precede Muslu' work as they take these to be constant and as such can assume a constant coefficient of discharge for the weir.

The definition sketches in Appendix B demonstrate how Muslu has gone about notating the characteristic parameters for side weir flow. These figures will help with understanding Table 3.1. This table is a comparison of many of the major empirical methods which have been formulated over the past 80 years. It demonstrates the large amount of variability which occurs between C_m, which is the discharge coefficient calculated from measured data and L/B, which is the geometric ratio of weir length divided by channel width.

Source	Equation	Froude Num.		L/b		p/h1		p in tests (m)	Cm in example
		Tests	Example	Tests	Example	Tests	Example		
Subramanya and Awasty (1972)	$C_m = 0.846\left(\frac{1-F_1^2}{1-F_1^2}\right)^{1/2}$	0.02-0.85	0.671	0.2-1.0	6.03	0.0-0.96	0.86	0.0-0.60	0.385
Nandesamoorthy and Thomson (1972)	$C_m = 0.288\left(\frac{2-F_1^2}{1+2F_1^2}\right)^{1/2}$	-	0.671	-	8.92	-	0.86	0.0-0.60	0.26
Ranga Raju et al. (1972)	$C_m = 0.54 - 0.40F_1$	0.1-0.5	0.671	0.1-0.7	8.54	-	0.86	0.2-0.5	0.272
Hager (1987)	$C_m = 0.485\left(\frac{2+F_1^2}{2+3F_1^2}\right)^{1/2}$	0.00-0.87	0.671	3.33	5.59	-	0.86	0.0-0.20	0.415
Sing et al. (1994)	$C_m = 0.33 - 0.18F_1 + 0.49\frac{p}{h_1}$	0.23-0.43	0.671	0.25-0.50	3.69	0.42-0.85	0.86	-	0.63
Jalili and Borghei (1996)	$C_m = 0.71 - 0.41F_1 - 0.22\frac{p}{h_1}$	-	0.671	-	9.42	-	0.86	-	0.246
Borghei et al. (1999)	$C_m = 0.7 - 0.48F_1 - 0.3\frac{p}{h_1} + 0.06\frac{L}{B}$	0.1-0.9	0.671	0.66-2.33	5.29	-	0.86	0.01-0.19	0.438

Table 3-1 - Side Weir Equations for Discharge Coefficients

Source: Muslu (2001)

Much of Muslu' (*2001*) paper is based on the work of De Marchi, where he analytically integrated Eq 3-21 to calculate the side weir discharge. In this De Marchi assumed that the C_w was a constant which allowed for a simple method of solution. It is this which Muslu (*2001*) contends is not strictly correct as C_w in fact a function of several other parameters, namely Froude Number, geometric ratio $\left(\frac{L}{b}\right)$ and the weir height divided by the energy head $\left(\frac{p}{H}\right)$.

$$-\frac{dQ}{ds} = q = \frac{2}{3}C_w\sqrt{2g}(h-p)^{2/3} \qquad \text{Eq 3-21}$$

Muslu (*2001*) determined that the coefficient of discharge is more accurately represented by Eq 3-22. Making C_w variable means that an analytical integration of De Marchi formula (*Eq-21*) is impossible, so a numerical technique was employed (*Muslu, 2001*).

$$C_w = 0.611\sqrt{3\psi z - 2} \qquad \text{Eq 3-22}$$

In which:

$$\psi = 1 - K(F) \quad \text{Eq 3-23}$$

$$z = \frac{h}{H} \quad \text{Eq 3-24}$$

In Eq-23 the value of K is a function of $\frac{L}{B}$, which is summarized in figure 7 of Muslu (*2001*). The value of K can be calculated using the standard equation of a straight line, as shown in Eq-25.

$$K = .0855\left(\frac{L}{B}\right) + .036 \quad \text{Eq 3-25}$$

This model is more robust than the methods represented in Table 3.1 as it accounts for the variance that can occur in C_w given a change in a number of parameters. As it is based on hydrodynamic principles, and not experimental work which has then employed a curve fitting technique to derive a formula, it is a far more efficient solution technique (*Muslu, 2001*).

3.3 Theoretical Methods

The models outlined above in section 3.2 are indicative of what experimental results will be compared to. It is hoped that this will shed some light on appropriate solution methods.

Once experimental results have been analysed using the software package Matlab, the situation will then be compared to the results that are gained when the situation is simulated using the models mentioned previously. Doing this will allow a direct comparison between theoretical and experimental values.

3.4 Experimental Considerations

This project required experimental work so that results can be compared to the theoretical methods available. One of the most important facets of the experiments is to find a way to determine the discharge of the main channel and the side weir accurately. The other requirement is that the change in momentum over the length of the weir needs to be determined.

With these considerations in mind a suitable experimental set up needs to be considered. As there is no flume capable of side weir experimentation at the university, an appropriate experiment needed to be designed and constructed. With the arrangement of the experiment such that:

- Weir discharge can be contained
- Weir lengths can be changed
- Velocities can be measured with precision at set locations
- Enough length in the flume to ensure minimal turbulence
- Water height can be adjusted for longer weirs
- Discharge can be measured for the entire flume

CHAPTER 4

4. EXPERIMENTAL TECHNIQUES

4.1 Initial Designs

The first stage of the project was to construct a flume capable of side weir experimentation as the university does not have anything suitable. Preliminary thoughts on the matter involved connecting a flume onto the reticulation system in the universities hydraulics laboratory. The idea was that this would allow an easy method of dealing with the water discharging from the side weir. Constructing an entirely new flume also had the added advantage of being able to install a false side which would allow for an efficient means of changing the side weir length.

It was thought that this would be the best way to approach the problem as it provided simple and efficient way of adjusting for different weir lengths. A major problem with this approach however, was going to be measuring velocities in a precise manner. This is critical in calculating a velocity profile at either end of the side weir.

As this approach would also require a considerable amount of construction and would be difficult in terms of taking measurements it was deemed that a new approach should be sought.

4.2 Experimental Flume

After some thought it was decided that the broad flume in the hydraulics laboratory could be used. This would involve constructing a narrow flume to sit in the broad flume and devising a way to contain all the flow within the narrow flume. The broad flume was appealing for several reasons:

- No concerns of containing side weir flow
- Smaller amount of construction needed
- Velocities could be precisely measured using the ADV which is primarily attached to the broad flume
- More cost efficient
- Flow meter is attached to the broad flumes main pump

For the above reasons it was decided to run the experiments within the broad flume as it was more than adequate for what was required.

4.2.1 Flume Design

The design for the narrow flume needed to be reasonably similar to that of the initial design in that it needed a false side or some other means of changing the weir length without having to move the entire flume. As the weir needed to be a sharp crested weir it also needed to be made of a material that could be milled, such as Perspex or steel.

Initially it was thought that Perspex would be the best option and it would be ideal if the entire flume was made from it, so that no changes in roughness occurred. After a costing of this it was quickly decided this would not be appropriate for this projects budget, seeing as one sheet of Perspex costs roughly $800.00 and two sheets would be required to have a flume the length of the broad flume.

Following discussions with workshop staff it was discovered that a square section of 10mm Perspex was available. This section was 300 x 300 mm, internal dimension, which was ideal to fit within the flume; the only issue was its length. As it was only a 2.4 meter long section, concerns were raised about the flow not being steady enough as it passed the side weir, which had the potential to cause erroneous results. It was decided that this section should be adequate so it was cut into a 300 x 200 mm flume, with the base being 300 mm.

To allow for different weirs to be installed an 800 mm slot was cut out 400 mm from the end of the flume. Initially it was hoped this could be a tongue and grove joint to prevent leakage and cause minimal disturbance to the water, however workshop staff advised that this would be difficult to mill. Therefore it was decided that the piece would be cut as a tight fit and a piece of Perspex secured to the outside of the channel to hold this section in place with a light silicon seal to keep it water tight (*refer figure 4.1*).

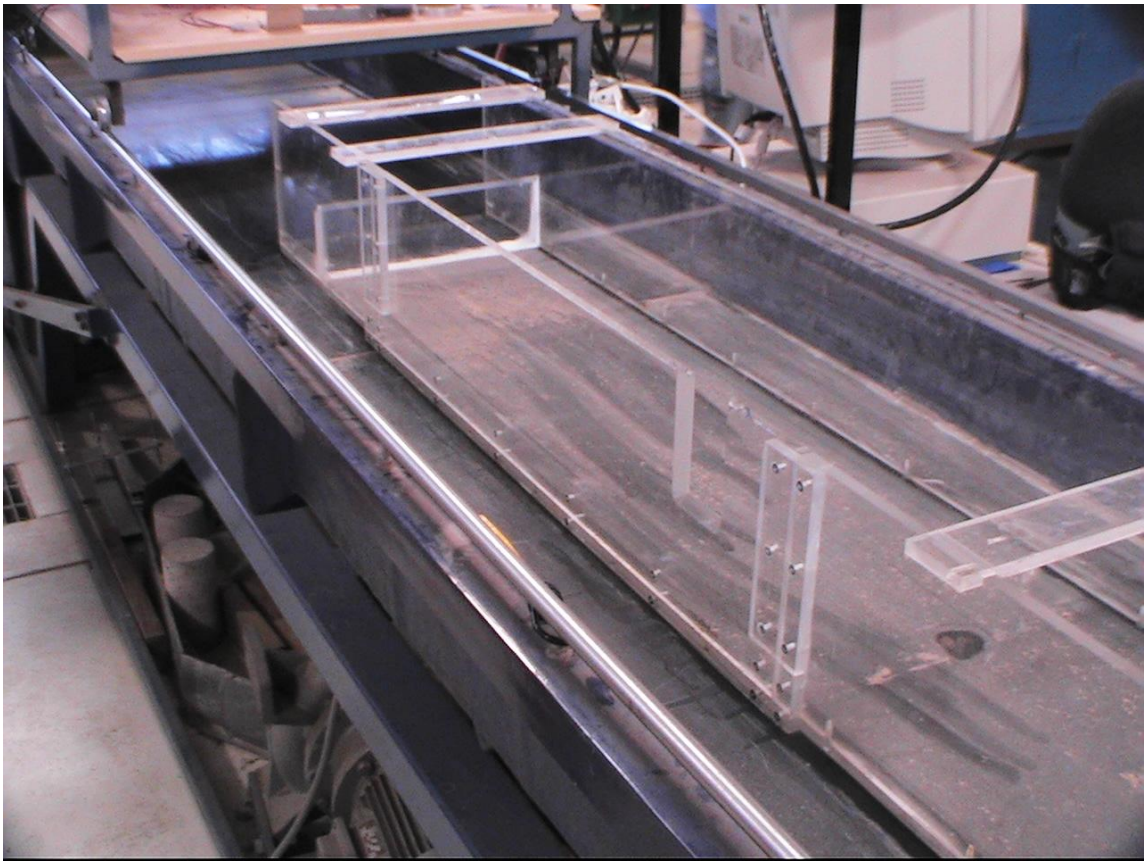

Figure 4-1 – Weir piece which can be removed to allow weir resizing

4.2.2 Controlling the Flow

The major issue with having a narrow flume sit inside the broad flume is that all the water from the intake needs to be directed down the narrow flume. An additional problem was that the side weir was at the same height as the broad flumes sides, so to achieve side weir flow water needed to be flowing at a height greater than the broad channels sides.

This was overcome by placing a box over the intake which increased the head of the channel (*refer figure 4.2*) and placing a weir at the end of the narrow flume to back the water up and create a subcritical flow regime (*refer figure 4.3*). Three sharp crested weirs were milled at heights of 100, 125 and 150 mm; this ensures that as the side weir length is increased the depth of the flow in the channel can be increased to create adequate flow over the side weir.

Figure 4-2 – Intake box to ensure flow is contained in narrow flume

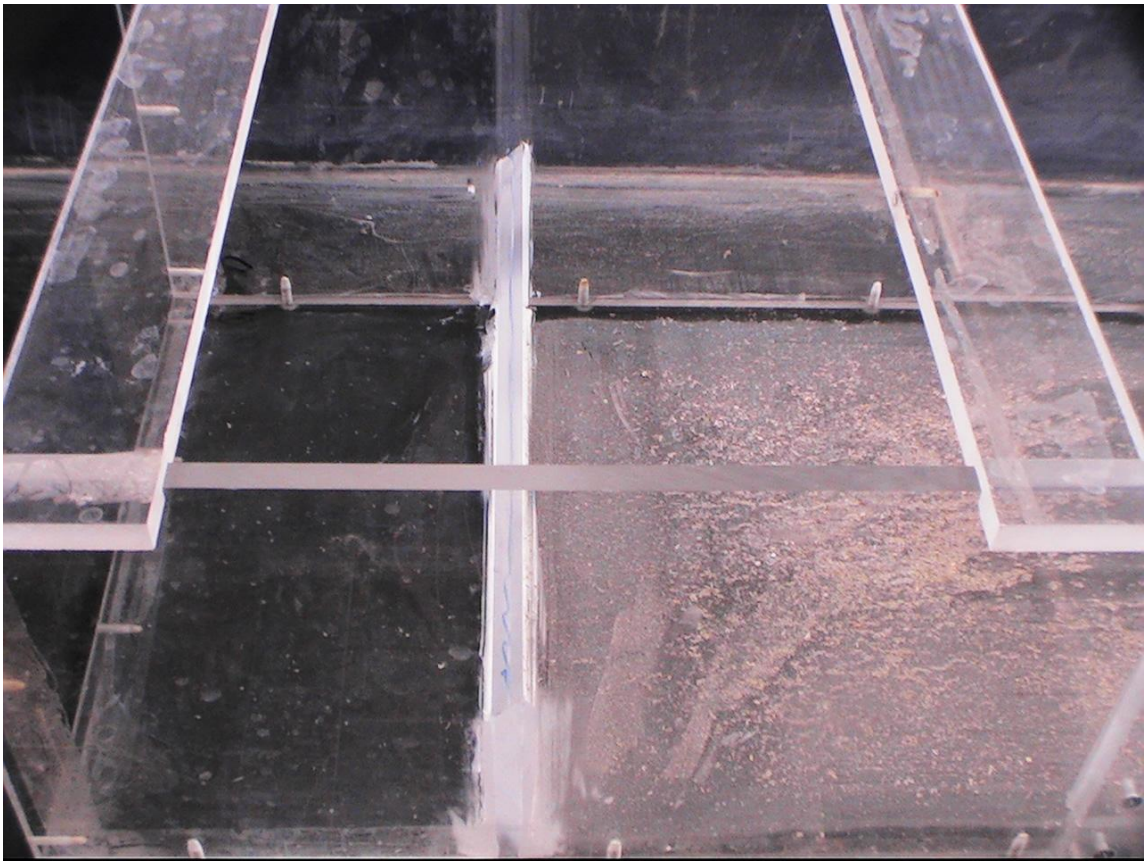

Figure 4-3 – Downstream weir to increase water level

As this box over the intake increased the total head of the water, a significant amount of energy is added to the water which is not needed. This energy causes big disturbance which creates a more turbulent flow. The added turbulence means that the water does not eject cleanly from the weir and actually clings to the outer face of the channel. This is demonstrated in figure 4.4 where it can be seen that the flow is clinging to outer channel face at the downstream end.

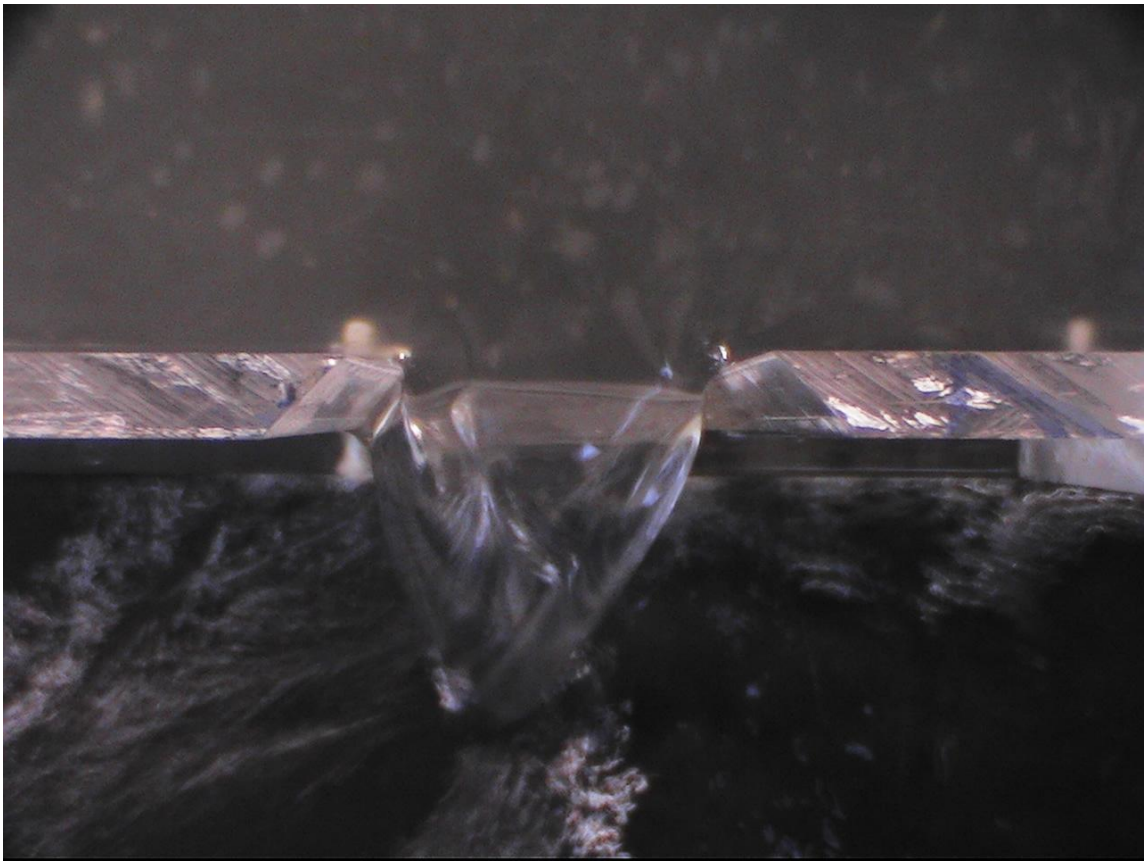

Figure 4-4 – Weir flow clinging to outer channel face

4.2.3 Stilling the Flow

To prevent this disturbance to the flow more intensive stilling measures were put in place. These measures needed to be quite extensive as the development length is rather short. The measures put in place include:

- Perspex Baffles
- 5 layers of fly screen
- 2 weirs and a sluice gate (*weir, sluice gate, weir*)
- 17 x 10mm holes in the box over the intake

All of these measures where contained in the first meter of flow and contributed to getting the flow to a steadier rate (*refer figure 4.5*). It could be seen that it was working because the water was cleanly ejecting from the side weir and velocity readings being taken were at a far more constant rate (*refer figure 4.6*). This can be seen when comparing figure 4.4 and 4.6

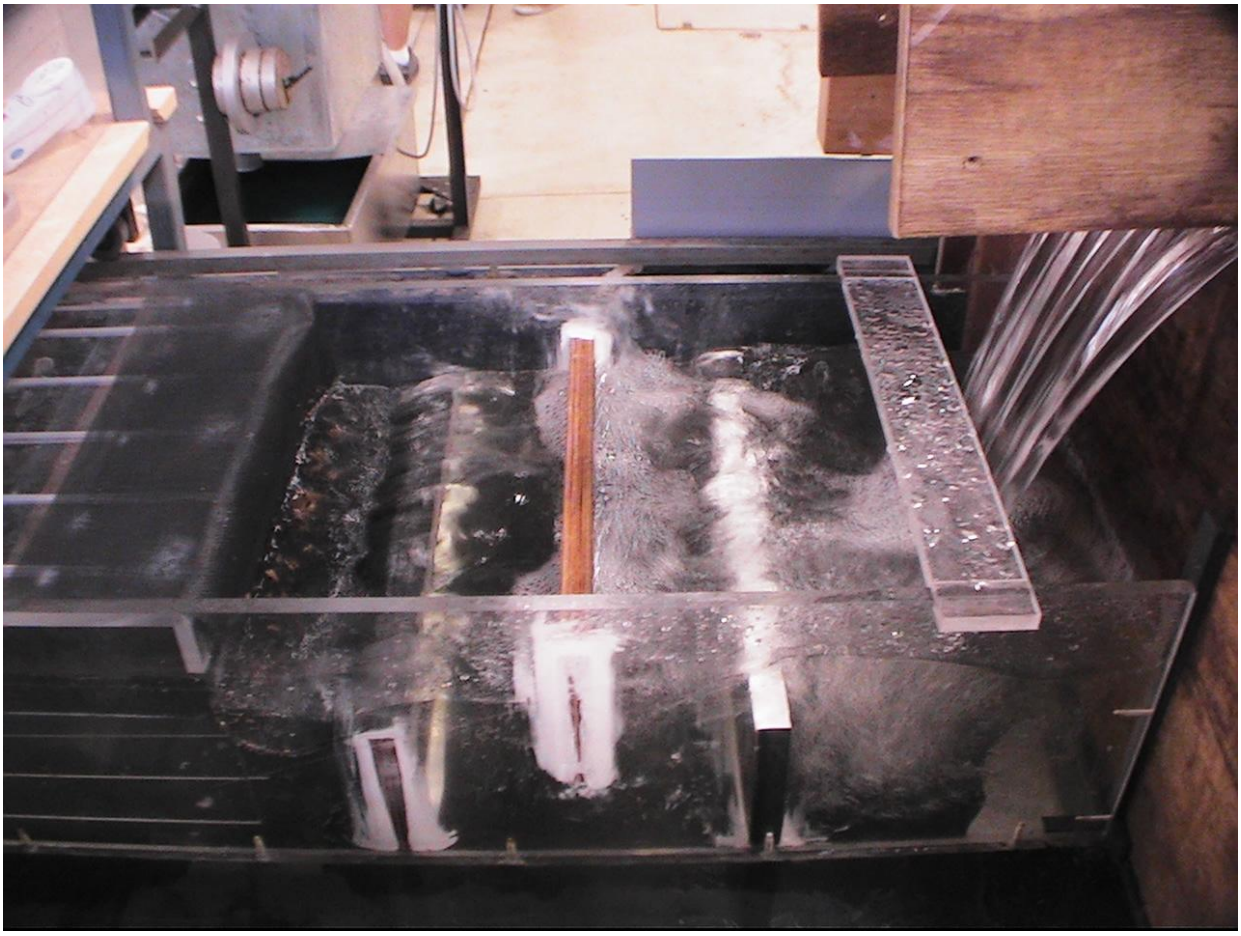

Figure 4-5 – Means of steadying the flow

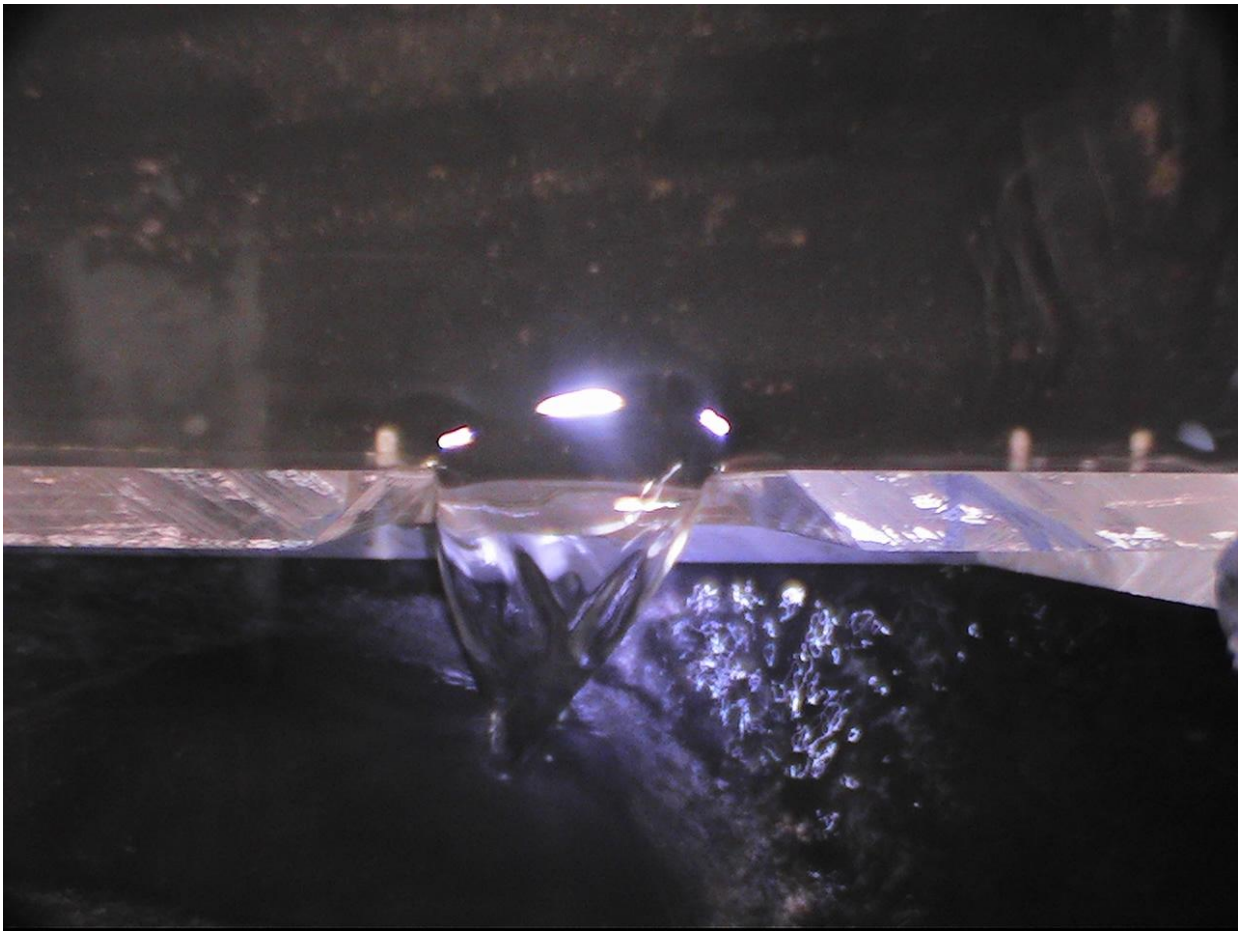

Figure 4-6 – Weir flow ejecting cleanly

4.3 Measurement Techniques

4.3.1 Acoustic Doppler Velocimeter

The Acoustic Doppler Velocimeter, or *ADV,* is a device used to measure point velocities within an open channel flow environment. The ADV can be used in conjunction with a 2 or 3 arm probe configuration. For these experiments the probe with the 3 arms was used, as it measures velocity in the three component directions, x, y, and z (*refer figure 4.7*).

Figure 4-7 – ADV probe

The ADV measures velocities by examining a sample volume, the size of which the user is able to select. It then emits out a sound wave of a frequency which is also able to be

elected by the user. The movement of this sound wave over the sample volume in the component directions, x, y and z is then converted to component velocities. Users are also able to select how many samples are to be taken.

In this set of experiments a 9 mm sample volume was used in conjunction with a 1Hz frequency. It was decided that 60 samples would be adequate to find the average of each component in the case of slight variations in the velocities. This meant that velocity readings took one minute to gather at each point

Using the ADV allows point velocities to be measured which will allow point momentum losses to be calculated across the length of the weir. This will demonstrate the fact that there is a net momentum change.

4.3.2 Angle of Discharge

To measure the angle of discharge several photographs will be taken of the side weir flow in plan view. These photographs are then imported into a drafting package such as AutoCAD 2010. Using such a package will then enable the angle of discharge to be determined to a higher precision than would be found by measuring it in the laboratory. This will be an important facet as the changing angle of the flow will be an interesting characteristic to compare between the discrete weir and the longer weir.

4.3.3 Flow Rate

The discharge, or flow rate, will be known for the flow at the upstream end of the side weir. This will be determined using the flow meter which is attached to the pump outlet. Knowing this flow rate will provide a way a validating the velocities being measured by the ADV.

4.3.4 Water Depth

Water depth has been measured in a rather crude form. Metal rulers were used to take the heights upstream and downstream of the weir. Initially it was hoped to take a water profile using a needle gauge, however setting this up would have taken some time. So it was decided because of time restrictions to use a simpler approach that would provide the essential information.

CHAPTER 5

5. EXPERIMENTAL RESULTS

5.1 Discrete Side Weir

The discrete side weir was the first to be tested. It was a 50 mm slot the with the weir crest sitting 100 mm above the channel bed. The purpose of testing this weir was to demonstrate the side weir characteristics, and seeing if these remained constant across the length of the weir.

Data from experiments has been analysed using a Matlab script, which is contained in Appendix C, and examines several aspects of the side weir flow, mainly:

- Velocity vectors
- Momentum change over the weir, longitudinal and lateral
- Velocity contour plot and extrapolation
- Mean section velocity
- Angle of discharge
- Calculated side weir discharge
- Flow conditions (*Reynolds number, Froude number*)

The main interest in this is examining the side weir discharge in comparison to theoretical methods. It is also important to confirm that there is a momentum change as water flows past the side weir.

5.1.1 Velocity Vectors

Velocity vectors have been determined using Matlab's quiver function. This function requires inputs of the position of the vector in x, y and z components and the velocity vector in x, y, and z components. The output of this function is in the form of a 3D graph such as figure 5.1, which is the velocity vector plot for the discrete side weir.

These vectors are a graphical representation of the data measured using the ADV, plotted in the location of measurement. Velocities were measured at three depths and across the channel in ten mm increment. Sixty sample velocities were taken for each component at each point; these were averaged to calculate x, y and z velocity components for each point.

This vector plot is used to validate the data that was measured and ensure that no outliers are in the data set, which is evident from this plot. If the plot above is rotated to so that it is a view of the x-y axis it can be seen that the vectors on the 70, 80 and 90 mm layers are almost precisely overlaid.

It is interesting to note the divergence of flow between 350 and 400 mm on the x-axis at 0 mm on the y-axis, this x-position being on the weir side of the channel and the y position being upstream of the weir. This is shows the flow starting to break away as some lateral momentum is clearly added to the water. At the same x position but at 90 mm on the

y-axis, immediately downstream of the weir, the flow has a significant vertical component. This can be explained as the flow trying to revert back to an equilibrium flow after a component of water was lost over the side weir.

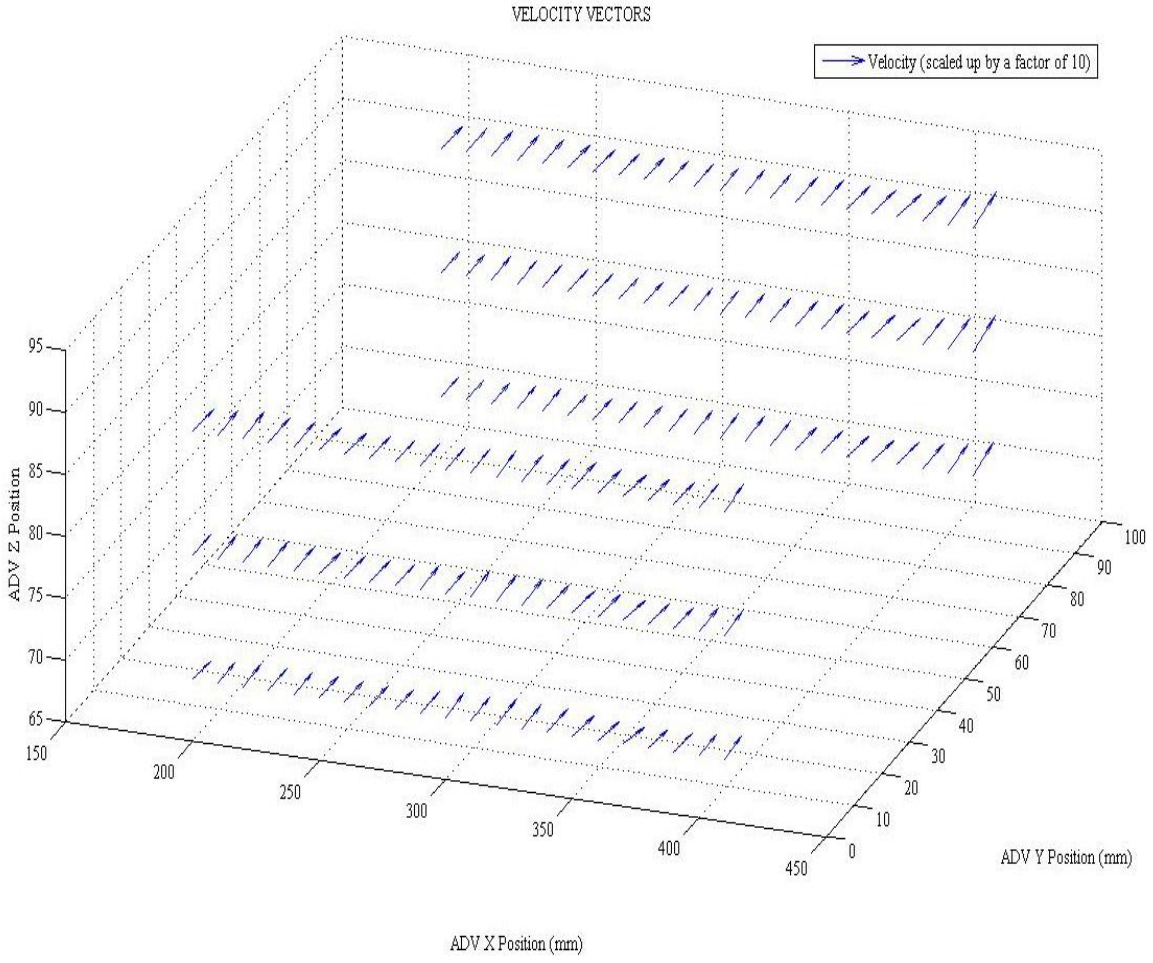

Figure 5-1 – Discrete Weir Velocity Vectors

5.1.2 Momentum Change

The change in momentum has been considered by examining point momentums upstream and downstream of the weir and then calculating the difference between them. For example if considering a point at 200 mm along the x-axis, 0 mm along the y-axis and 90 mm along the z-axis; then it would be related the same point but at 90 mm along the y-axis. This treats the flow as stream lines and examines how the momentums of these change over the length of the weir.

Momentum at a point has been calculated using equation 5.1, which gives the momentum in terms of a force (*N)*. The value calculated can then be used to find the difference between two points on the same streamline. This has been done to calculate changes in momentum in the lateral and longitudinal flow.

$$F = \rho QV = \rho V^2 A \qquad \text{Eq 5-1}$$

Figure 5.2 shows these longitudinal momentum changes for the points in each layer of the z-axis and also has averages of the momentum changes for those layers. No clear trend is evident among the layers, however if examined as a whole it does seem to trend upward with progression to the right. This indicates that momentum is being lost, however on the weir side of the channel there is a slight momentum gain. A gain at this point could be caused by the relatively large body of water trying to fill the space left by the flow that ejected out the side weir.

The average for the channel is a loss of momentum which supports the argument that Chow (1959) was wrong to drop the term which contained the change in discharge. However, because of the erratic nature of the graph it is thought to be inconclusive.

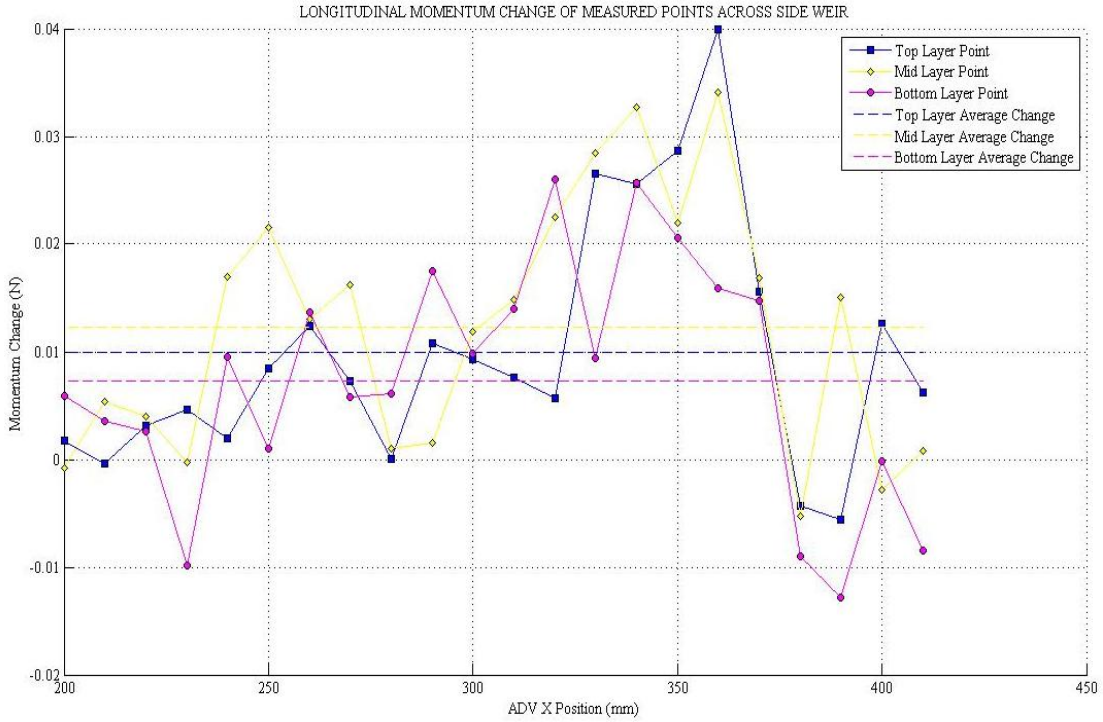

Figure 5-2 – Longitudinal Change in Momentum for Discrete Weir

Figure 5.3 shows the lateral momentum change over the side weir. This was plotted by calculating the momentum change in the x direction between the upstream and downstream points. It shows clearly that there is a significant amount of momentum being gained near the side weir, *in proportion* to the other side of the channel. The average change in momentum for the channel was an increase in momentum in the lateral direction.

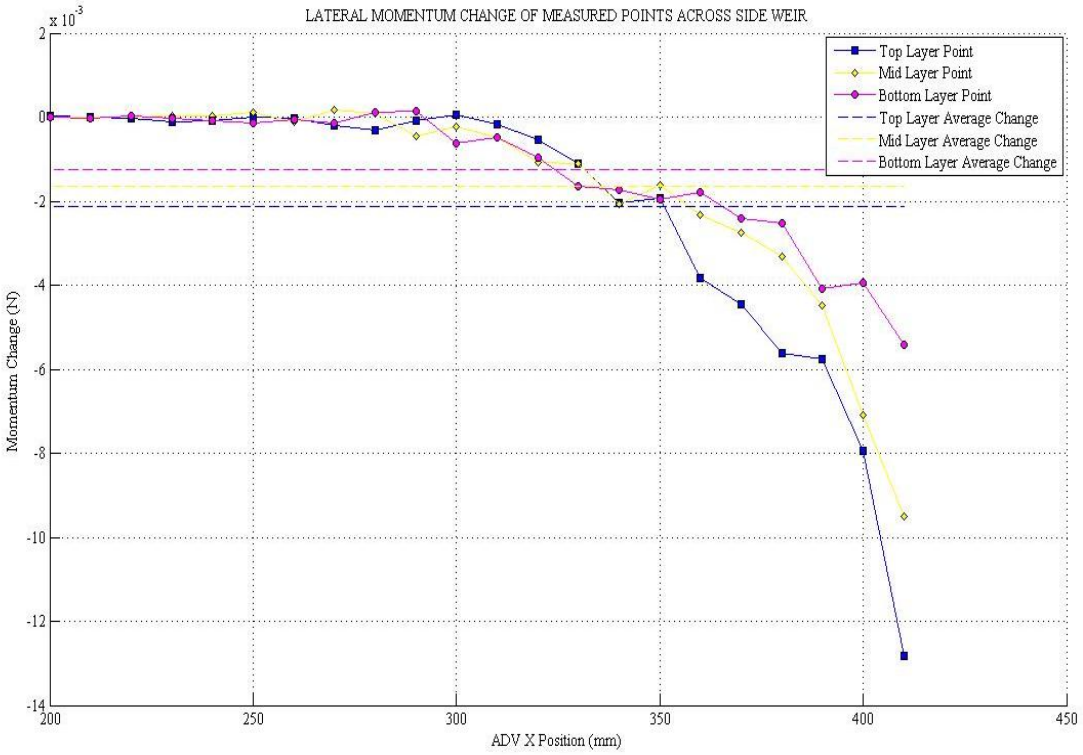

Figure 5-3 – Lateral Change in Momentum for Discrete Side Weir

5.1.3 Velocity Contours

It was necessary to create a contour plot of the velocity for two reasons:

- Velocities on the very edges of the flume couldn't be measured
- Measuring the entire depth was too time consuming

The plot is effective as it gives a visual profile of how the velocity acts across the channel and is also able to extrapolate velocities for uncalculated regions. Having a full velocity profile is important for the ensuing calculations.

Figure's 5.4 and 5.5 show the distribution of velocities at sections upstream and downstream of the side weir. This is an important factor as the uneven distribution of velocities dictates how hydraulic theory can be applied when analysing the problem.

These plots were achieved by creating a mesh grid which extrapolated data from the points which already had experimental velocities assigned to them. This allowed a full section velocity to be calculated with reasonable accuracy. The velocities were calculated on a 2.5 mm grid, which means that velocities are known across the entire section at 2.5 mm increments. The experimental velocities used were the y components as the change in this component indicates exactly how much flow has been lost.

A reason that these plots may be slightly inaccurate is that the velocity above the highest measured point in the flow, which was at 90 mm in the z position, will actually decrease. It has been shown that the free surface velocity in open channel flow is in fact less than the velocity of the water just below the surface (Chadwick et al., 2004). These points along the water surface could not be measured with the 3 dimensional probes as the entire probe would not be submerged; however with the right probe configuration these free surface velocities could be measured with the 2-dimensional one.

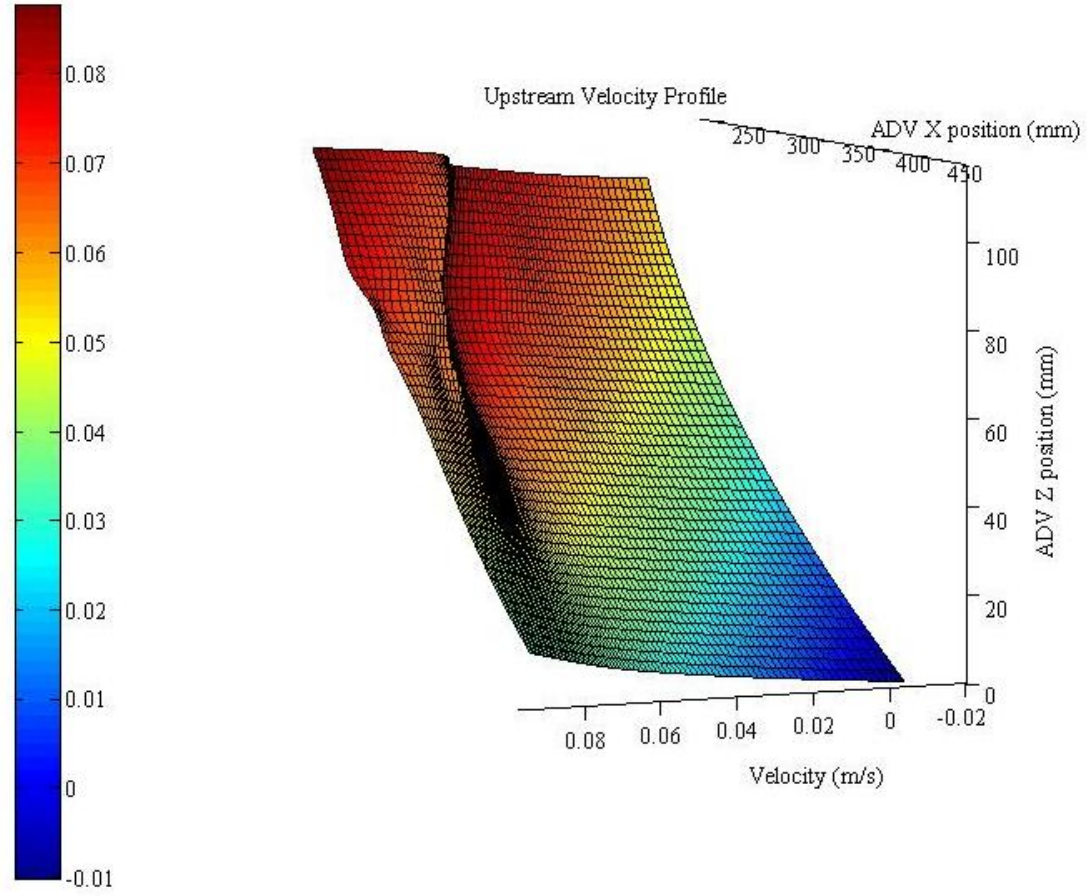

Figure 5-4 – Upstream Velocity Contour/ Surface Plot

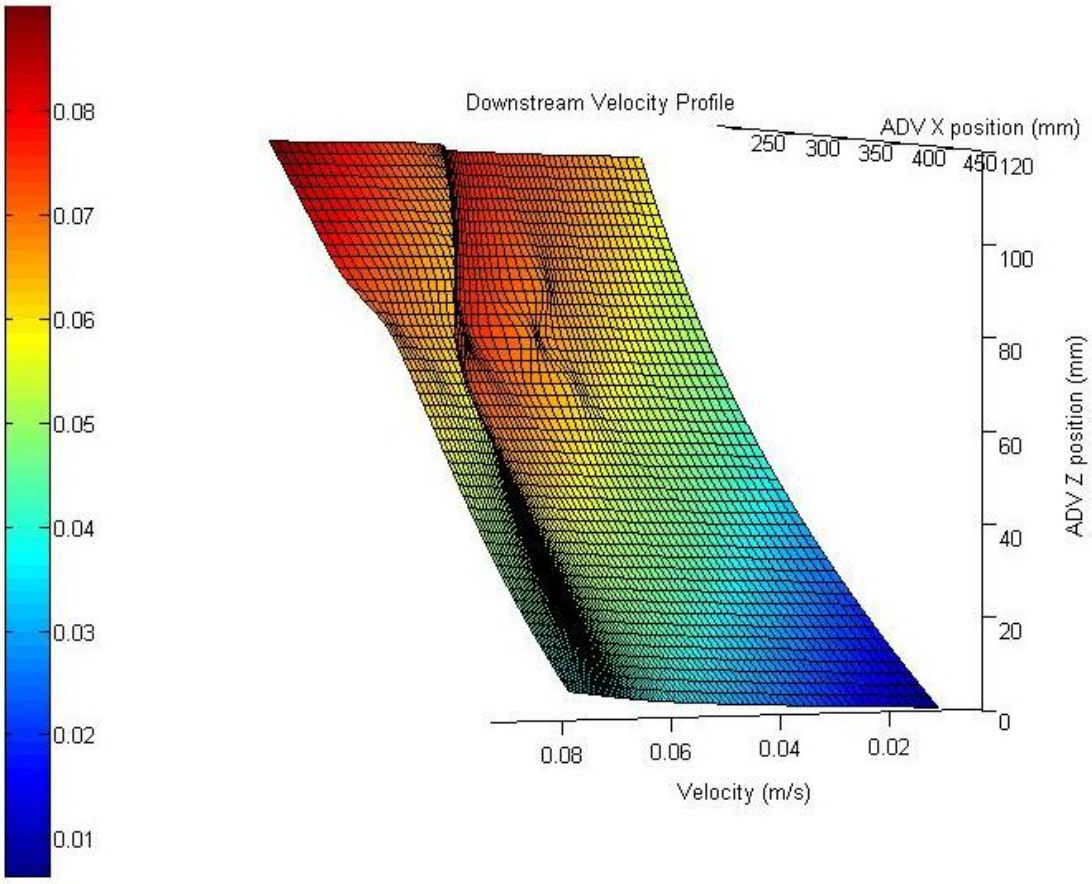

Figure 5-5 – Downstream Velocity Contour/ Surface Plot

5.1.4 Mean Section Velocity

The mean section velocity is important as continuity requires the average velocity be used in conjunction with area and discharge. Using the grid data formulated to produce the contour plots, the mean section velocity could be calculated. This was done by taking the mean of the entire array which returned mean values for each column of velocities, then by taking the mean of these values the mean section velocity was found.

This process is scripted into the Matlab program. For the section upstream of the weir a velocity of .0542 m/s was calculated and downstream a velocity of .0563 m/s was found. It was unexpected that the downstream velocity is greater than the upstream, this could be an error of measurement, or an error in the extrapolation (i.e. needed more velocity points).

5.1.5 Angle of Discharge

The angle of discharge is an important characteristic of the side weir problem. It has a direct relationship with the longitudinal velocity and can be used in conjunction with that to determine the velocity of the water ejecting from the weir.

Measuring the angle of the discharge of the discrete weir shows clearly that it is not a constant value. With the angle upstream 31 degrees from perpendicular and the downstream angle 8 degrees anti-clockwise from perpendicular. This implies that the angle is decreasing along the weir which means that there is more lateral momentum acting on the flow the further downstream the weir that is being examined. This means that discharge

is not a constant for the entire length of the weir and is in fact increasing with each step downstream.

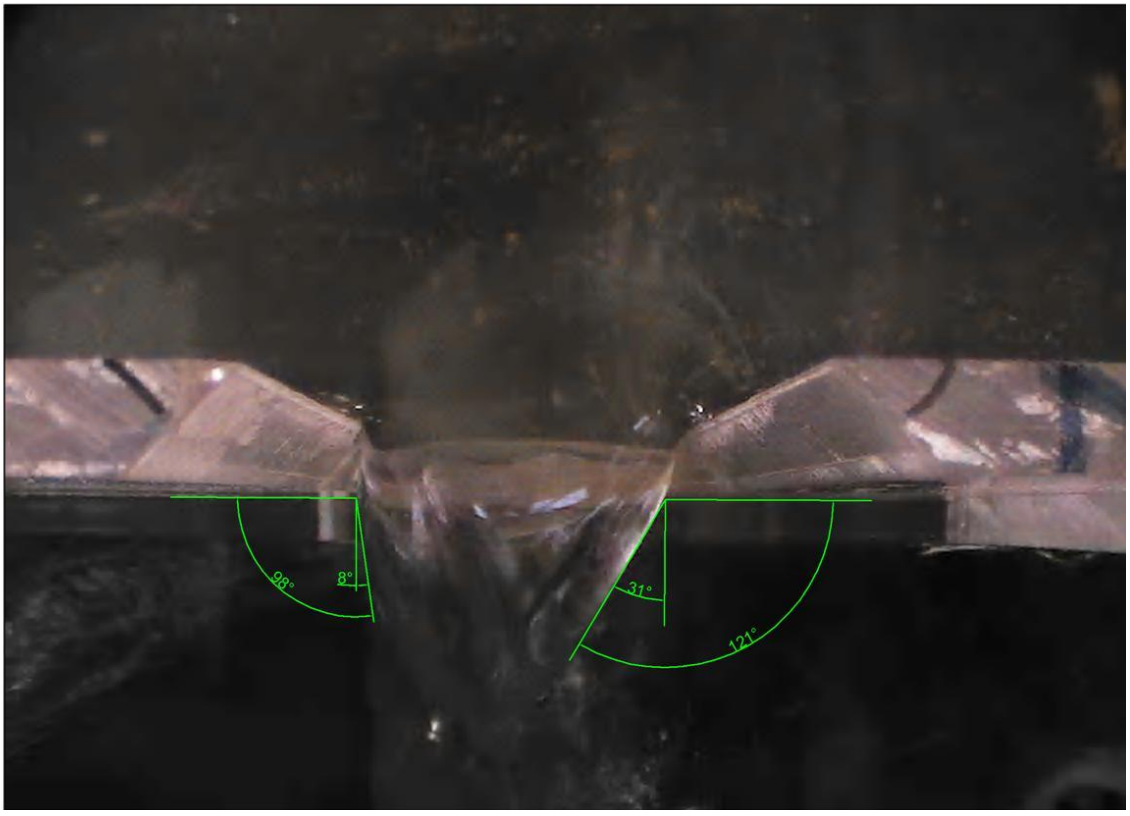

Figure 5-6 – Discrete Weir Angle of Discharge

5.1.6 Side Weir Discharge

There are two ways of measuring the side weir discharge, either using the difference in discharges calculated from the mean section velocities or, by using the flow rate determined using the flow meter which is on the outlet of the pump and the angle of discharge. Using both will serve as a validation and highlight any experimental error.

Both of these discharges are calculated in the Matlab script. The discharge based on the velocity profiles is calculated by using the mean section velocities to find flow rates upstream and downstream of the weir. These flow rates are then subtracted from one another to give a discharge for the side weir. The discharge was calculated by the Matlab script as being -.00013 m^3/s, this is obviously wrong as this implies water is being added to the channel which is clearly not the case.

The Matlab program is calculating this value correctly as the downstream velocity is higher than upstream, which would correlate to the resulting side weir discharge. The most likely cause for this error is either an experimental error or an error relating to the extrapolation of the measured velocity points. It is most likely that the measured points did not extend deep enough into the water profile, which has not allowed the exact shape of profile to be calculated.

By using the angle of discharge the weir discharge can also be calculated. This method is still going to be unreliable as the mean section velocity downstream of the weir will still need to be used. If the error is contained in the downstream velocity then it will also be carried into this discharge calculation.

The upstream velocity for this calculation was found using the channels flow meter, which for the side weir experiments was reading 140 L/min. This was first converted to litres per second and then divided by the upstream area to give a velocity of .0654 m/s which is greater than the calculated mean section velocity of .0537 m/s. The value of .0654 m/s this can be used in conjunction with the downstream velocity of .0563 m/s and the angle of discharge which taken at an average is 23 degrees.

Using Eq 5-2 a velocity of .0656 m/s was calculated for the velocity of the side weir flow. This can be converted to a discharge by using the height of flow over the weir, which was 119 mm upstream and 122 mm downstream. The calculated discharge was found to be .000395 m^3/sec, which is equivalent to .395 L/sec. This answer seems reasonable for the 50 mm discrete weir however because of uncertainty surrounding the mean section velocities it is hard to be sure.

$$V_1 + V_2 = 2V_j \cos\theta \qquad \text{Eq 5-2}$$

5.1.7 Flow Conditions

It is important to characterise the flow conditions as it will determine how the flow is considered by certain theoretical applications. The two main considerations are the Reynolds number, which classifies the mixing of the streamlines, and the Froude number, which indicates the flow regime.

For the discrete weir a Reynolds number of 1720 was calculated. This means the flow is turbulent according to the classification that flow with a Reynolds number of greater than 1000 is turbulent.

The flow regime has been classified based on the Froude number. It was found that a Froude number of .061 existed upstream of the weir which indicates flow is subcritical. This means that the normal depth of flow is above the critical depth, and that the velocity is less than celerity. Knowing this means that the experiment was run under the right conditions as supercritical and critical flows fall outside the scope of this project.

5.2 Long Side Weir

The long side weir was the first to be tested. It was a 300 millimeter slot the with the weir crest sitting 100 millimeters above the channel bed. The purpose of testing this weir was to make a comparison with the discrete side weir, and examine it with reference to the theoretical analysis as the channel width is the constraining factor of the side weir length in many of the empirical approaches.

Data from experiments has been analysed using a Matlab script, which is contained in Appendix C, and examines the same aspects of side weir flow looked at in the discrete weir experiments.

5.2.1 Velocity Vectors

The velocity was measured for the long weir in the same manner as the discrete weir; measurements were taken at 20 mm increments in the x direction, 10 mm increments in the z direction and 140 mm increments in the y direction. The x position spanned the entire measurable width of the channel, while the z position started from when the probe was just below the water surface to a point 20 mm below this. Measurements in the y direction started at a point just upstream of the weir, then mid weir, and finished with measurements downstream of the weir.

Figure 5.7 is a plot of the velocity vectors for the long weir experiment. As with the discrete weir the velocities are plotted at the point where measurements were taken at in the flume. This figure clearly shows a divergence of roughly half the flow, this was expected as

the weir is the same length as the channel width. Seeing this would imply that the discharge of the side weir will be around half of the upstream discharge.

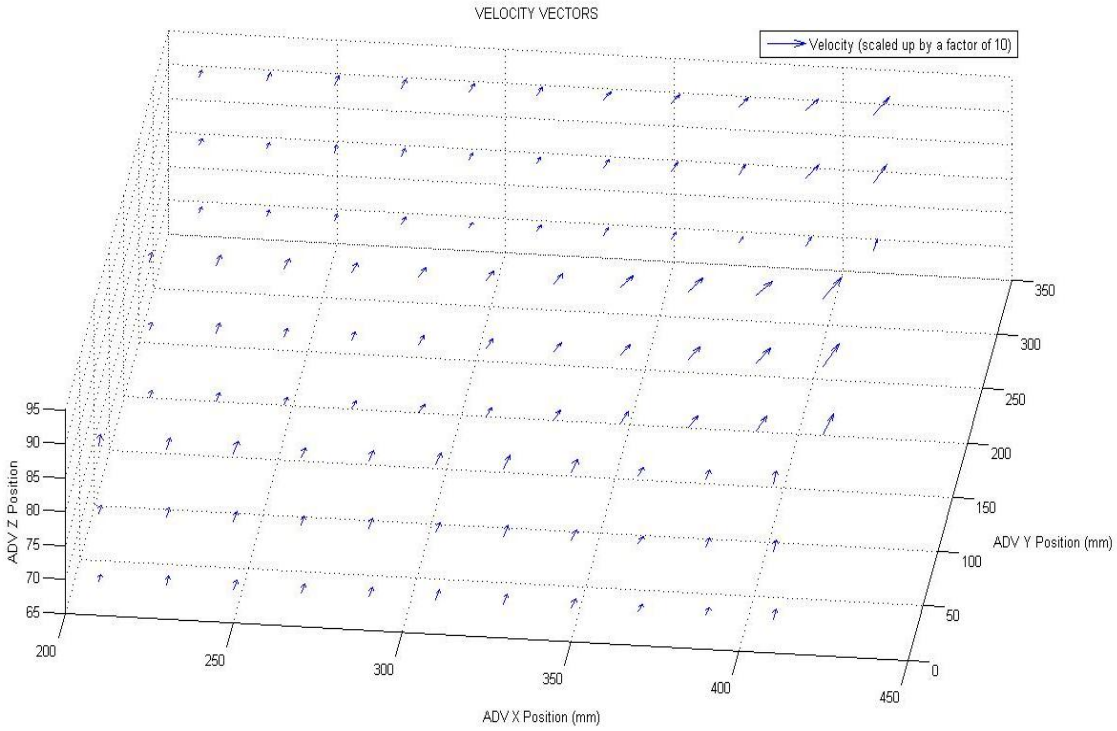

Figure 5-7 – Long Weir Velocity Vectors

In figure 5.7 there is a much larger z component to the velocities near the side weir. This is due to the fact that much more water is being drawn off over the side weir, which would result in a momentum gain in the z direction as well.

5.2.2 Momentum Change

Momentum change has been calculated using the same method outlined in section 5.1.2. The following figures are in the same format as those presented in section 5.1.2, and even though velocities were measure in the middle of the weir these have been considered.

Figure 5.8 shows the longitudinal momentum change. It is interesting to note that in comparison with Figure 5.2 that the long weir momentum change has a clear trend which is followed by all layers.

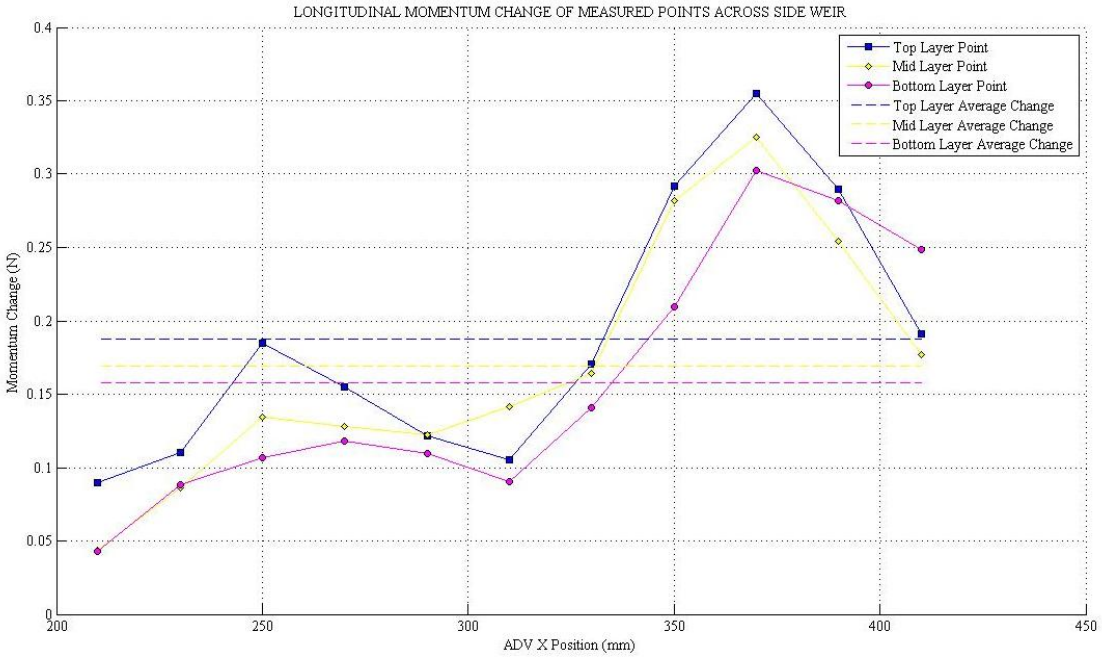

Figure 5-8 – Longitudinal Change in Momentum for Long Weir

In Figure 5.8 the trend is following a clear path, which was to be expected. This is vastly different from figure 5.2 which is very erratic in contrast. The momentum change for the long weir is expected to be more clearly defined though, as the change is far more

prevalent due to the fact more water is discharging via the side weir. It is interesting to note that the greatest change does not occur to the far right of the channel where the weir is but is in fact offset to the left a little bit. This could be viewed as conformation that the discrete weir change longitudinal momentum plot (Figure 5.2) is accurate as it had a similar trend, although not as clearly defined.

Figure 5.9 shows the lateral momentum change over the length of the long side weir. This follows the same trend as seen in Figure 5.3, but with a greater magnitude. The bottom layer of measured point here is not experiencing the gains seen in the other layers. This would imply that the deeper the measurements are taken the less lateral momentum gain would occur. This makes sense as the side weir location means that only the top portion of flow is dramatically affected. That would imply that velocity measurements taken closer to the channel base would result in momentum gain approaching zero in the x-direction.

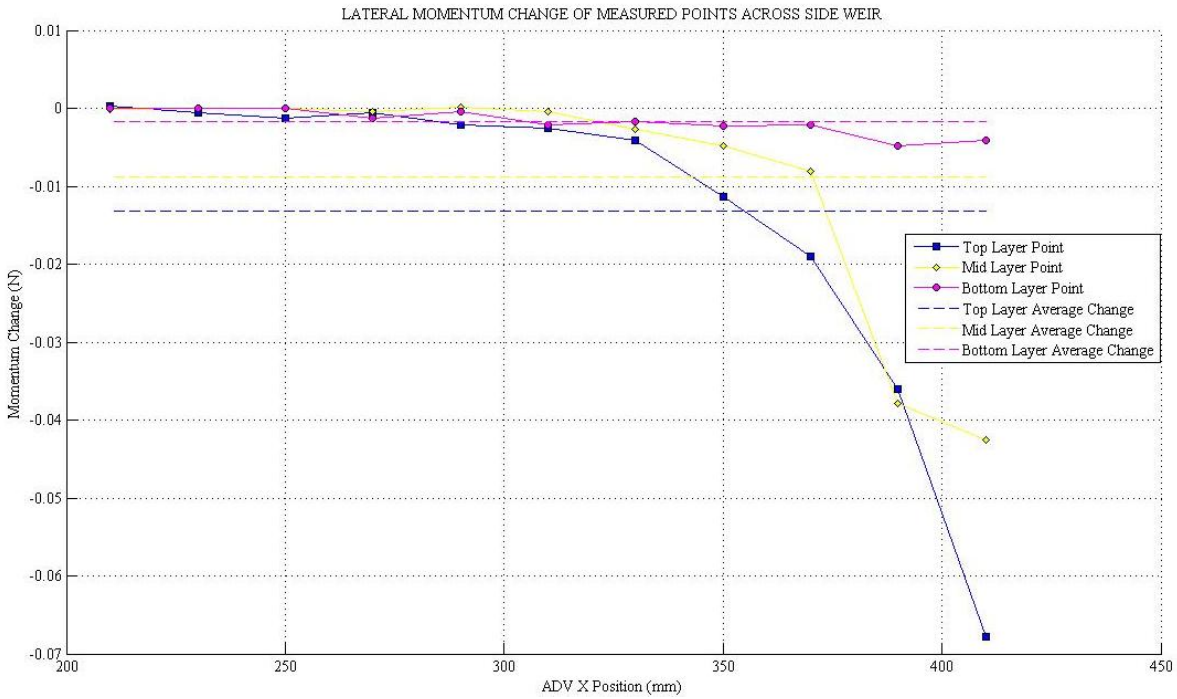

Figure 5-9 – Lateral Change in Momentum for Long Weir

The results for the change in momentum for the long weir are particularly conclusive. Especially for the longitudinal momentum loss, this shows that if momentum isn't being added to the water it does not mean that there is no momentum change.

5.2.3 Velocity Contours

The contour plots for the long side weir were compiled using the same method outlined in section 5.1.3. It can be seen that these contours have predicted at negative velocity in the bottom right hand corner. This is unlikely, particularly for the upstream velocity profile. What has probably occurred is that the measured velocities did not extend

deep enough and the velocity profile is not a true representation how the velocities change throughout the section.

This means that if the velocity appears to be dropping off quite significantly in the top section of the channel, where the velocity measurements were taken, then the extrapolation will conform to these rates of change. It is most likely that this has resulted in the negative velocities.

Apart from this discrepancy with the rate of change over the channel cross section, the contours seem to be plausible. There is a distinct change in maximum velocity between Figures 5.10 and Figures 5.12; this is to be expected with much greater discharges occurring with the long side weir.

These plots also show how the velocity magnitude changes across the channel section before during and after the side weir. A shift is noticeable as the velocity goes from being greatest in the centre of the channel upstream, then more concentrated to the right of the channel at the mid weir section and heavily skewed to the left of channel downstream of the weir.

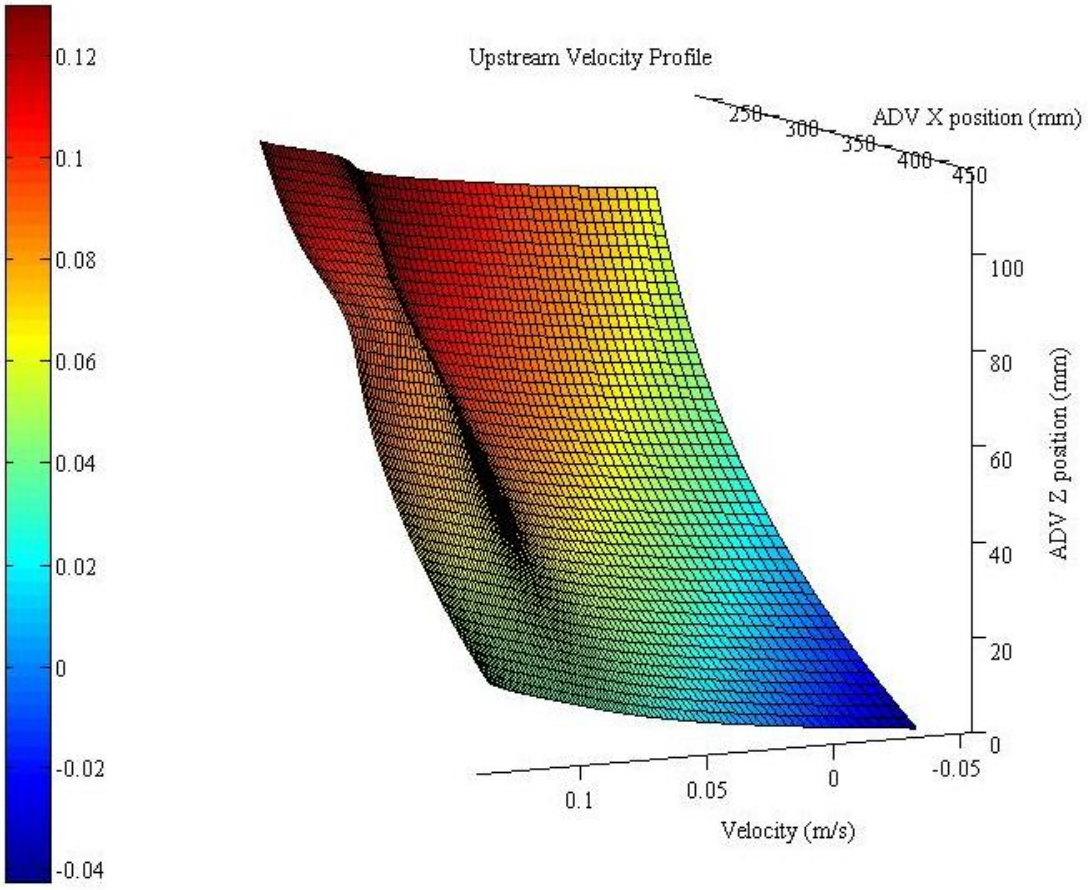

Figure 5-10 – Upstream Velocity Contour/ Surface Plot

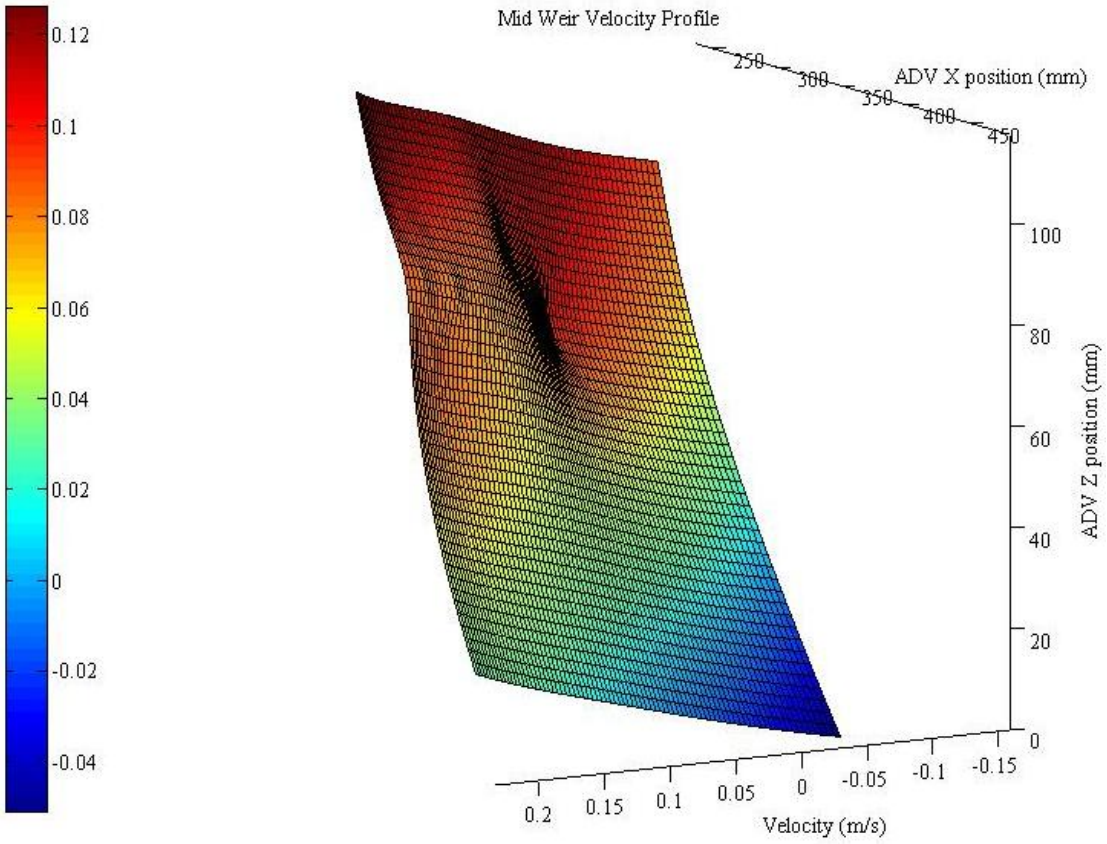

Figure 5-11 – Mid Weir Velocity Contour/ Surface Plot

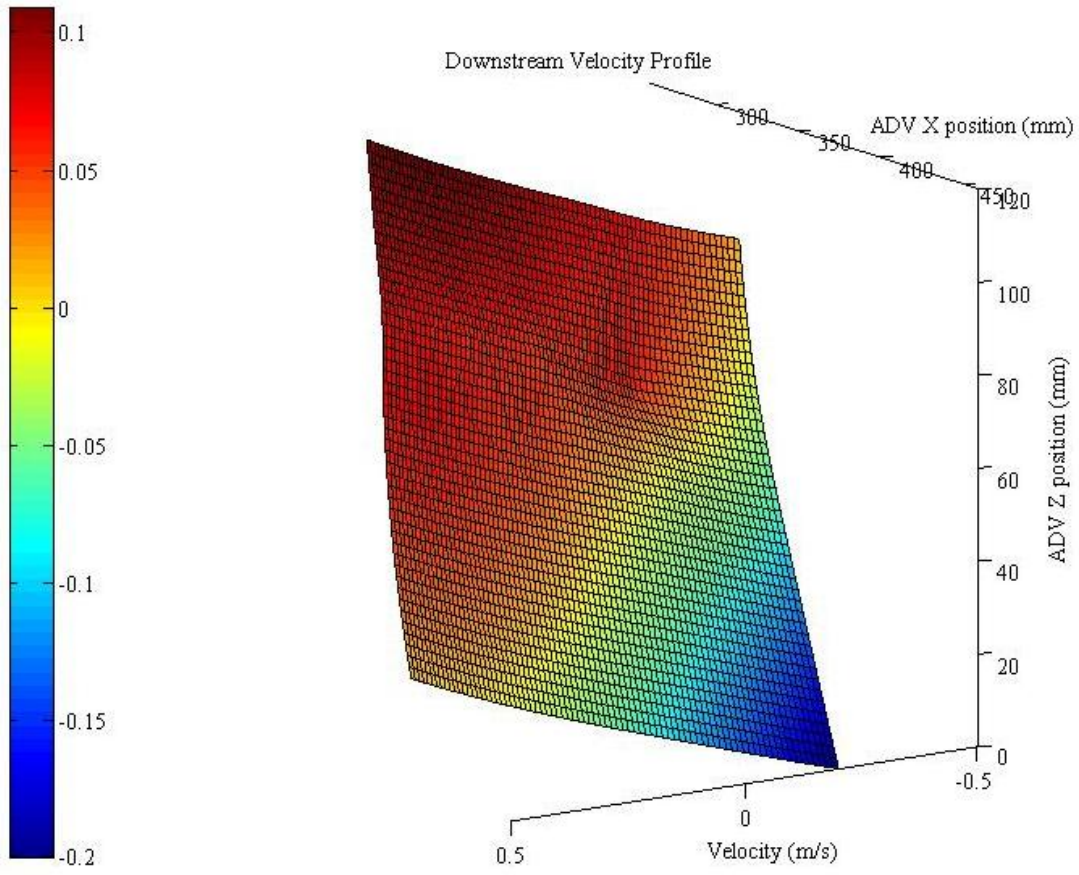

Figure 5-12 – Downstream Velocity Contour/ Surface Plot

5.2.4 Mean Section Velocity

Mean section velocity is calculated by the Matlab script, as mentioned in section 5.1.4. The mean section velocities for each cross section are outlined in Table 5.1 below.

Measurement Point	Mean Section Velocity (m/s)
Upstream of Weir	*0.0721*
Mid Weir	*0.0622*
Downstream of Weir	*0.0163*

Table 5-1 – Long Weir Mean Section Velocities

Table 5.1 shows that the velocities are decreasing with progression down the weir. This is the expected result and seems far more accurate than those for the discrete weir. It is interesting that a significant proportion of the velocity upstream remains at the mid weir point. This would indicate that the velocity loses momentum at an exponential rate.

5.2.5 Angle of Discharge

As with the discrete weir, the angle of discharge is not constant. In fact it has a greater variance across the length of the long side weir. This was to be expected though as there is a longitudinal momentum loss and lateral momentum gain, which results in the increased angle of discharge.

The measured angles can be seen in Figure 5.13 below. It should be noted that the flow had a tendency to cling to the outer wall of the channel in this experiment. The most likely cause of this is a chip out of the downstream corner of the side weir. This weir was

not milled as precisely as was hoped and as such the results have probably suffered. Time constraints meant that another test could not be performed and as such the angle may in fact be greater than was measured at the downstream end.

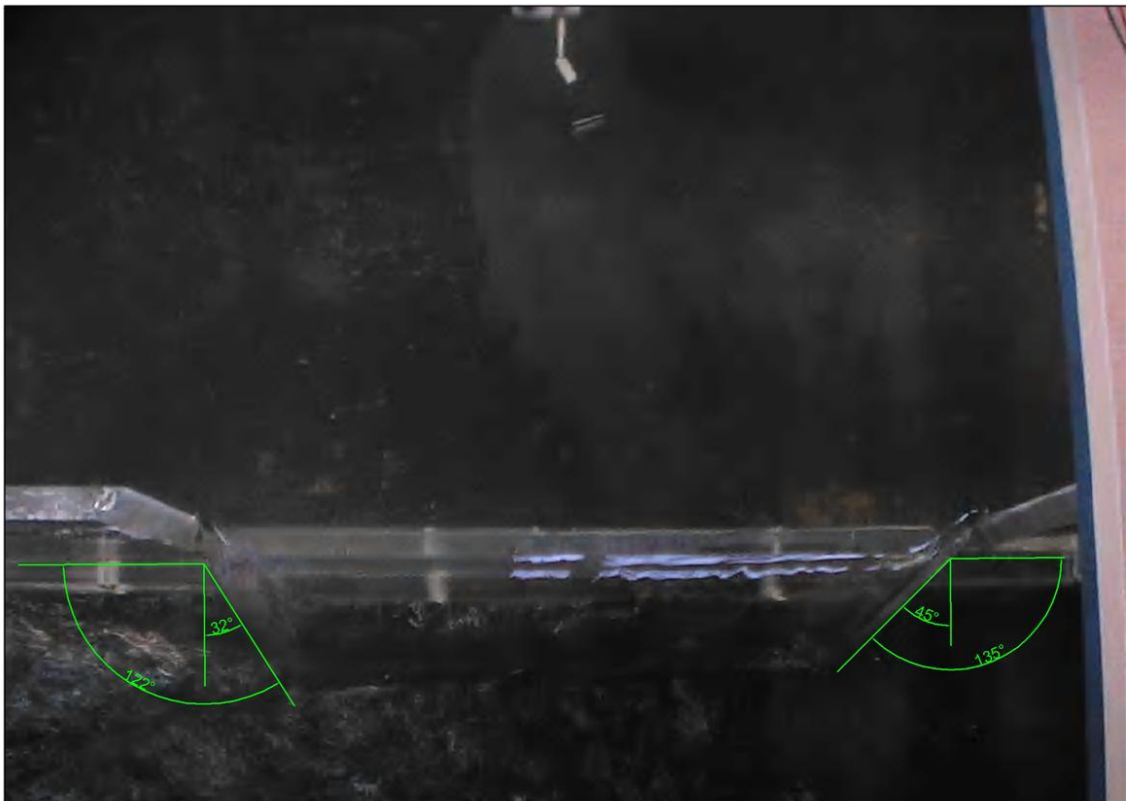

Figure 5-13 – Long Weir Angle of Discharge

5.2.6 Side Weir Discharge

The side weir discharge has again been calculated using two methods as was done with the discrete weir. A discharge of .0020 m^3/sec was calculated using the difference in the upstream and downstream discharges which were found by using the mean section velocities. Using the flow meter discharge and the angle of discharge a side weir discharge of .0020 m^3/sec was calculated. As these values match up it can be assumed that this data is reliable enough to be compared with the theoretical methods.

There is still the possibility of error in these results as the flow meter was fluctuating from 192 L/min to 200 L/min. 195 L/min was used in calculations as it was deemed to sit around this value for the majority of the experiments. It is likely that an error is contained in the mean section velocity calculation, which would be carried through to the side weir discharge calculation.

5.2.7 Flow Conditions

For the long weir a Reynolds number of 2397 was calculated. This means the flow is turbulent according to the classification of flow, in an open channel with a Reynolds number of greater than 1000, is turbulent.

The flow regime has been classified based on the Froude number. It was found that a Froude number of .0853 existed upstream of the weir which indicates flow is subcritical. This means that the normal depth of flow is above the critical depth, and that the velocity is

less than celerity. This means that the experiment was run under the right conditions as supercritical and critical flows fall outside the scope of this project.

5.3 Results Discussion

From the results obtained an opinion has been formed about the experiments and their accuracy. It is the general line of thought that they have not been as successful as was hoped. The main problem has lain in the precision to which they have been conducted; with short cuts taken to save time having a big effect on accuracy.

The biggest problem with the results has been the mean section velocities. Having a velocity profile it was hoped that the change in velocity over the length of the side weir would be easily determinable. However, it was found that because the velocity readings were not taken to a sufficient depth, the rate of change of the velocity was most likely not properly obtained. This has resulted in what is believed to be an over estimate of the mean section velocity, as was seen with the downstream mean section velocity in the discrete weir experiments.

Another possibility is that an error has been contained in the positioning of the ADV. The ADV has an offset distance of about 10 mm when reading velocities, this was not taken into account when it was being positioned and so there is a possibility that the velocities recorded, particularly the downstream readings, actually having a component of the reading contained in the weir section. This would lead to skewed and inaccurate results.

The error could also lie in the fact that the water was not still enough for the experiments. Any large variations in the flow could potentially skew the data set, which would lead to errors. In saying this the velocities did seem reasonably consistent, and aligned with expectations.

Another issue that arose during the experimentation process was manufactured parts that were not of a high enough quality. The main instance of this was with the long weir piece, which had chips in the corner of the weir crest and it was not milled to an even point across the length. It is thought that this is the main cause of the flow clinging to the outer edge of the channel in the long weir experiments. This would have compromised the angle of discharge measurement.

As the discharges calculated in the discrete weir experiments do not align, there is no way of validating the results and as they need to be used with caution. The discharges calculated for the long weir experiment do match but as there are thought to be errors in the process these also need to be used carefully.

The experiments would have benefited from a complete depth profile being taken at the velocity cross section and of the side weir. This would have allowed for a more complete comparison with the direct step method proposed by Chow (1959) and with Muslu (2001). It was not imperative however it would have acted as a form of validation.

One or all of these issues discussed may have impacted on the experimental results; however one positive has arisen from the experiments. The momentum change was quantifiable over the length of the weir and as such it can be seen that Chow (1959) was wrong to drop the change in discharge from the derivation of the momentum equation when examining lateral outflow.

CHAPTER 6

6. THEORETICAL ANALYSIS

6.1 Lateral Flow Model

As was mentioned in chapter 3, an empirical method of solution has been developed by Ramamurthy and Carballada (1980). It is thought that this is one of the more accurate empirical methods available as it is based in the theory of free efflux which was presented by McNown and Hsu (1951). This section will examine a model that was constructed using the theory presented in lateral flow model, which was outlined in chapter 3. The results of this will be used comparatively with the experimental results.

The model was constructed in a Microsoft Excel spreadsheet which is shown in Appendix D. It used the same set of circumstances that were present in the experiments and utilised some of the data that was gained to ensure the circumstances being examined were the same. Both the discrete and long weir cases were examined as a way of determining the range of situations which the theory is applicable for.

Using this method with the same conditions that were present in the discrete and long weir experiments yielded discharges for the side weir. For the discrete weir the model predicted

a discharge of .233 L/sec, and for the long weir a discharge of 1.308 L/sec was calculated. These results have been tabulated in Table 6.1 below, with the results from the experiments included as a means of comparison.

Method	**Discharge (L/sec)**
Experiment (Long Weir) Mean Section Velocities	2.00
Experiment (Long Weir) Angle of Discharge	2.00
Lateral Flow Model (Long Weir)	1.308
Experiment (Discrete Weir) Mean Section Velocities	-.133
Experiment (Discrete Weir) Angle of Discharge	.395
Lateral Flow Model (Discrete Weir)	.233

Table 6-1 - Experimental Results and Lateral Flow Model Comparison

6.2 Lateral Inflow vs. Lateral Outflow

Chow (1959) presented theory on lateral inflow and outflow, which has been examined in chapter 3. As was mentioned there this theory is contentious, so both the inflow and outflow equations have been examined. The thought is that the inflow equation should hold true for the outflow case, as there is momentum being lost in the outflow case which would just result in a change of sign not ignoring the change in discharge term completely.

Therefore both the inflow and outflow equations were examined using the same parameters as the experimental set up. Both the discrete and long weir cases were examined. For the discrete weir a discharge of .330 L/sec was calculated using the inflow equation and .337 L/sec using the outflow equation. As this solution uses a direct step technique a plot of the weir water surface profile as calculated by both equations was also possible; this is shown in Figure 6.1.

The water surface profile plot is interesting as the inflow equation predicts a greater difference in the upstream and downstream water heights, which coincides with the measurements taken during the experimental process, with an upstream height of 119 mm and downstream height of 122 mm being recorded. This graph would imply that the inflow equation has the more accurate prediction based on these facts alone.

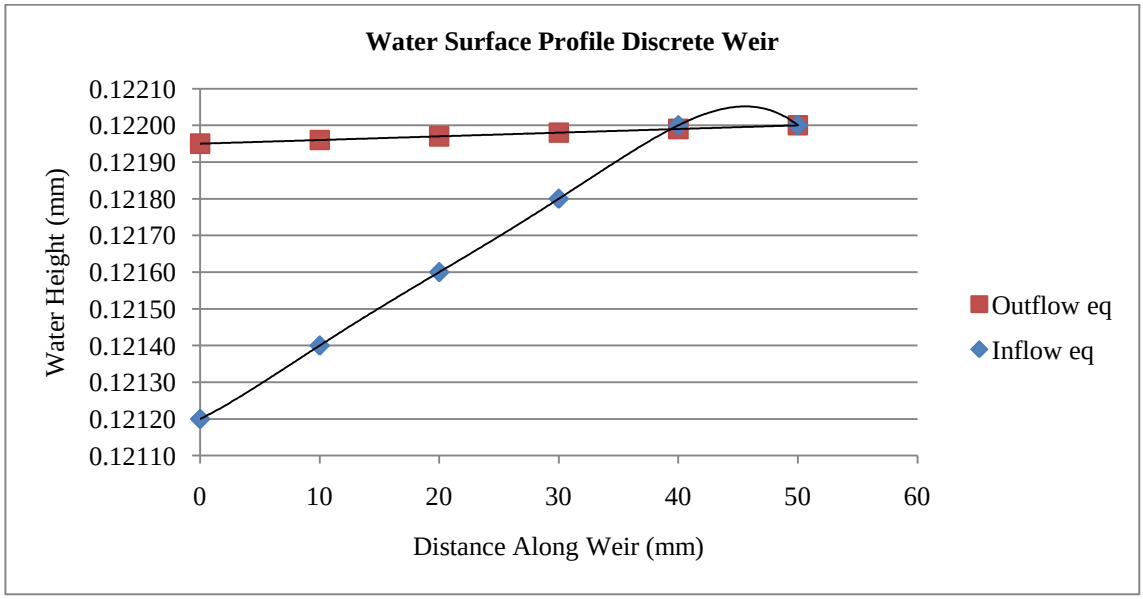

Figure 6-1 – Discrete Weir Water Surface Profile

For the long weir situation this method calculated a discharge of 1.669 L/sec using the inflow equation and 1.665 L/sec using the outflow equation. This shows that there is not a great deal of difference in the methods, however there is the possibility of erroneous results. The possible errors are in the bed slope, which was calculated based on experimental data and not measured, or the water heights which were not measure by an accurate method.

As with the discrete weir, a plot of the weir water surface profile was compiled to show the differences in the two methods. This is shown in Figure 6.2 below, and it can be seen that the inflow equation predicts a higher water surface profile in opposition to that of Figure 6.1 where it predicted a smaller one.

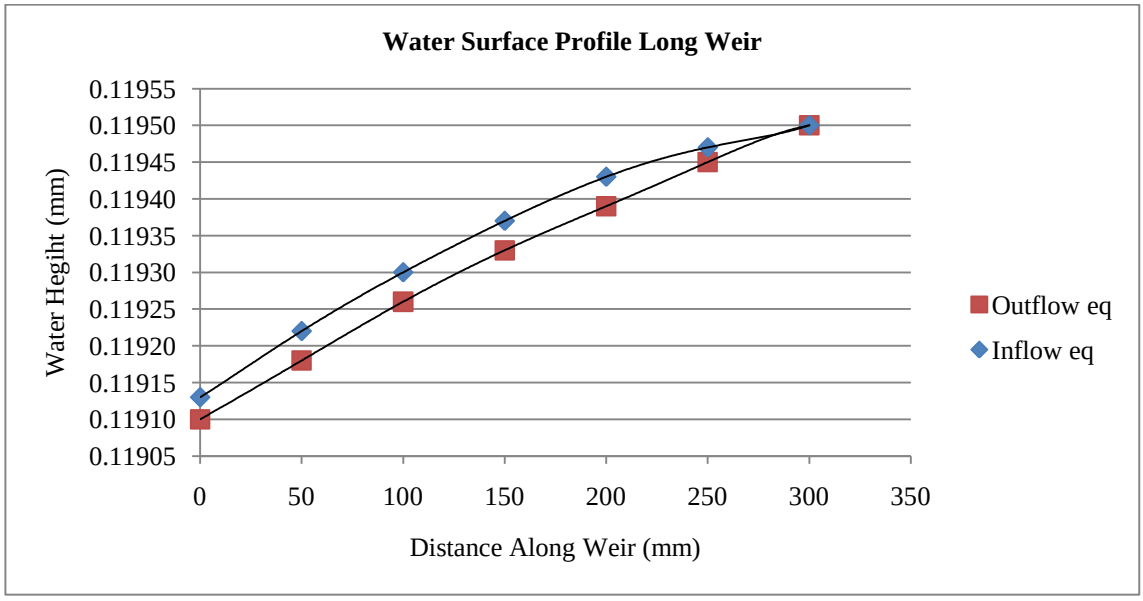

Figure 6-2 –Long Weir Water Surface Profile

Table 6.2 below, summarises the results of this method with comparisons to the experimental results. It is interesting to see that the inflow method calculates a higher discharge in one instance but lower in the other. The spreadsheets for this analysis are contained in Appendix D.

Method	**Discharge (L/sec)**
Experiment (Long Weir) Mean Section Velocities	2.00
Experiment (Long Weir) Angle of Discharge	2.00
Inflow Method (Long Weir)	1.669
Outflow Method (Long Weir)	1.665
Experiment (Discrete Weir) Mean Section Velocities	-.133
Experiment (Discrete Weir) Angle of Discharge	.395
Inflow Method (Discrete Weir)	.330
Outflow Method (Discrete Weir)	.337

Table 6-2 – Experimental Results and Lateral Flow Model Comparison

6.3 Numerical Analysis

Muslu (2001) uses a numerical approach to model the side weir problem. This method is examines the coefficient of discharge as an entity which changes across the length of the weir. To do this the changes in the water surface profile across the weir are taken into account as one of the major determining factors. As limited water surface profile data was taken this means that a complete comparison with this method is not possible.

This method is presented in a confusing manner and not much sense could be made of it. A summary of what could be determined was shown in chapter 3 which included a table of comparison of some existing methods of solution. The solution method looked promising however it could not be worked to get results which match up with the experimental data and the other methods. With a more thorough examination this method would be useful, however time restrictions meant that it could unfortunately not be used.

6.4 Results Discussion

The theoretical analysis was not as comprehensive as was originally hoped for however it was not completely unfruitful. The techniques that were examined shed some light on the side weir problem.

Ramamurthy and Carballada (1980) who presented the lateral flow model have established a technique which is good as a general solution. It is easy to use and computes values for side weir discharge with little difficulty, however in comparison with the experimental results it seems to be underestimating the discharge. This is undesirable as any designs based on this method will be potentially under designed.

Chow (1959) who formulated the lateral flow equations has a technique which is more mathematically sound than Ramamurthy and Carballada (1989) Lateral Flow Model. There was some contention surrounding the formulation of the outflow equation, and based on the results of the experiments it has been determined that the inflow equation should be used for the outflow equation as there is clearly a change in discharge. There is no reason warranting the dQ term being dropped in the derivation of the outflow equation and as such the inflow and outflow equations should be the same.

It can be seen from the results of the theoretical analysis that the inflow and outflow equations produce results in a very similar range. It is important to note that having the dQ term present in the derivation of the inflow equation will mean that it is going to be the more accurate method of solution. This is why it is recommended in as the equation to be used when solving side weir problems.

The results for the lateral flow equations do not align precisely with the experimental values. This can possibly be attributed to inaccuracy in the experimental process which led to miscalculated side weir discharges.

Muslu (2001) Numerical Analysis for Lateral Weir Flow seemed to be a promising piece of work, however the structure of the solution method is not made clear. It appeared to be heavily reliant on the changing heights throughout the channel, of which not enough experimental data was recorded. This meant that comparison to this method would be difficult.

One point of interest is the comparison Muslu (2001) made between many of the existing calculation methods. It highlights the difference in answers gained by techniques which are supposed to calculate exactly the same thing. The summary showed how using the same weir height, upstream water height and Froude number, gave a vast array of results using the different theoretical methods.

The results have been very inconclusive as no real comparisons could be made with the experimental data because there were too many errors. This means it is undeterminable as to which method is best. Assuming that the experimental discharge values are in the right order it would have to be said the Chow (1959) has a reasonably good solution. This is based on the fact that it is simple and easy to use with very few limitations.

CHAPTER 7

7. CONCLUSION

Side weirs have been the focus of extensive research in the past; however there is still no agreeance on what the best solution is. Each researcher who delves into the topic seems to formulate their own opinion on what the most important aspects of side weir flow are. This has caused a variety of solution techniques to be available, of which none seem to come to similar figures as was shown by Muslu (2001).

In the initially stages of this research the opinion was held that the angle of discharge was the defining parameter. This is still the opinion held however no conclusive evidence could be found to support this fact. The experiments were error ridden in part and thus made comparisons with the theoretical data practically impossible.

The need for precise and rigorous measurement technique in the experimental process has been highlighted. This is shown by the fact that when trying to extrapolate data to determine a mean section velocity, the water surface was predicted as having the highest

magnitude velocity; which we know in fact does not occur. Errors such as this could have been overcome by collecting more data points.

It was shown however that there is a distinct change in momentum over the length of the side weir. This evidence shows that Chow (1951) statement about there being no momentum being added to the water in the outflow case is correct. This still does not justify dropping the term containing the change in flow as water is being lost from the channel. This means that momentum is being lost over the course of the weir, so it is concluded that a change of sign in the dQ is all that would be required. Therefore it is the held opinion that the inflow equation presented by Chow (1951) is more suitable for solving side weir problems.

All of the theoretical approaches which were examined provided inconclusive findings as to which is the most appropriate method. Chow (1951) provided a technique which is simple and produces results similar to those obtained from the experiments. Although the results obtained from the Lateral flow model are still in the same vicinity as the experimental results they are not as close as Chows results.

Table 3.1, presented by Muslu (2001) best summarises a majority of the theoretical approaches to side weir flow. This shows the number of methods which have been formulated and the distinct variance in solution method and results obtained. All of the results are similar but each method is different in some way, and as such not all that robust. None of these methods seem to provide a clear solution to the problem; however Ramamurthy and Carballada (1980) have provided a method which is workable and reasonably robust.

The theoretical approaches are all so similar and close that further research would be required to acquire any conclusive findings. It is recommended that computer modeling using a program such a fluent may give clues as to what might be the correct solution technique. The following are recommended in any future theoretical investigations that take place:

- Comparisons need to be made with accurate experimental data.
- In the instance where experimental data is inconclusive or unavailable, a highly precise computer modeling program such as fluent could be employed as a means of comparison.
- Examining the effects of a wider range of parameters.

Further work is also required in obtaining experimental data. This would allow a validation of current data, as the experimental data gained in the course of this project is deemed to be erroneous and as such unusable to an extent. Future experimental work would need to be more rigorous and performed to a higher degree of accuracy. Recommendations for further experimental work include:

- Measure full depth of channel to ensure the rate at which the velocity changes over the channel section is accurately obtained.
- Measure water depth profile to a high precision at cross sections where velocities are calculated.
- Use a longer development length to ensure flow is still when the side weir is reached.
- Ensure manufacturing is performed to high standard, especially when weir pieces are milled. Any chips out of the sharp crest will compromise results.

This dissertation has examined methods of solution for the side weir problem based on theory found during a literature review. An experimental flume was constructed for the specific purpose of side weir experimentation. The experiments allowed the measurement of velocity profiles, side weir discharge and discharge angle; however it did not allow accurate enough means of water depth to be taken. This is in part due to time restrictions as setting up a means of doing this would have compromised the completion of the dissertation.

An attempt has also been made to validate the theory available, however incomplete and inaccurate data from the experimental work has hindered this process. As time was not permitting no attempt was made to formulate and validate a more complete method of solution. This means of the objectives set in Appendix A the four main points have been met, with objectives 5 and 6 not being attempted due to time restrictions and inconclusive results

8. REFERENCES

Chadwick, A, Morfett, J & Borthwick, M 2004, *Hydraulic in Civil and Environmental Engineering*, 4th edition, Spon Press, Milton Park

Chow, V 1959, *Open-Channel Hydraulics*, McGraw Hill, New York

Hamill, L 2001, *Understanding Hydraulics*, 2nd Edition, Palgrave Macmillan, New York

Nalluri, C & Featherstone, RE 2001, *Civil Engineering Hydraulics*, 4th edition, Blackwell Science Carlton Victoria.

McNown, J & Hsu, E 1951 "Application of Conformal Mapping to Divided Flow" *Proceedings of the 2nd Midwestern Conference on Fluid Dynamics*, Michigan, pp. 142-155

Ramamurthy, A & Carballada, L 1980 "Lateral Weir Flow Model" *Journal of the Irrigation and Drainage Division*, ASCE, Vol. 106, No. 1, pp. 9-25

Collinge, V 1957 "The Discharge Capacity of Side Weirs" *ICE Proceedings*, ICE, Vol. 6, No 2, pp. 288-304

Hager, W 1987 "Lateral Outflow Over Side Weirs" *Journal of Hydraulic Engineering*, ASCE, Vol. 113, No 4, pp. 491-504

Ackers, P 1957 "A Theoretical Consideration of Side Weirs as Storm-Water Overflows" *ICE Proceedings*, ICE, Vol. 6, No 2, pp. 250-269

Muslu, Y 2001, "Numerical Analysis for Lateral Weir Flow" *Journal of Irrigation and Drainage Engineering*, Jul/Aug 2001, pp. 246-253

Appendix A

PROJECT SPECIFICATION

Appendix A

University of Southern Queensland

FACULTY OF ENGINEERING AND SURVEYING

ENG4111/4112 Research Project
PROJECT SPECIFICATION

FOR: **David Selwyn ROWLINGS**

TOPIC: AN EXPERIMENTAL AND THEORETICAL ANALYSIS OF SIDE WEIRS

SUPERVISOR: Prof. Rod Smith

PROJECT AIM: To use experimental data to validate available theoretical approaches to solving side weir problems, and determine if these are appropriate techniques.

PROGRAMME: **(Issue A, 7 March 2010)**

1) Research available literature on side weirs and lateral flow; and find appropriate theoretical methods to solve side weir problems.

2) Design and construct an experimental flume to enable side weir experimentation.

3) Test side notches of various lengths using flows of different depths and velocities; taking measurements of (i) discharge of main channel and side weir (ii) velocity profile of main channel (iii) side weir discharge angle (iv) slope of channel (v) depth profile of channel and, (vi) depth profile of side weir.

4) Investigate and attempt to validate theoretical approaches from (1) in comparison with experimental results.

As time permits:

5) Attempt to formulate a more accurate theoretical approach *(only if found theoretical approaches are questionable).*

6) Determine accuracy of formulated approach using the experimental flume.

AGREED _____ (*student*) _____(*supervisor*) _____ (*supervisor*)

Date: / /201 Date: / /2010 Date: / /2010

Examiner/Co-examiner: _____

Appendix B

DEFINITION SKETCHES

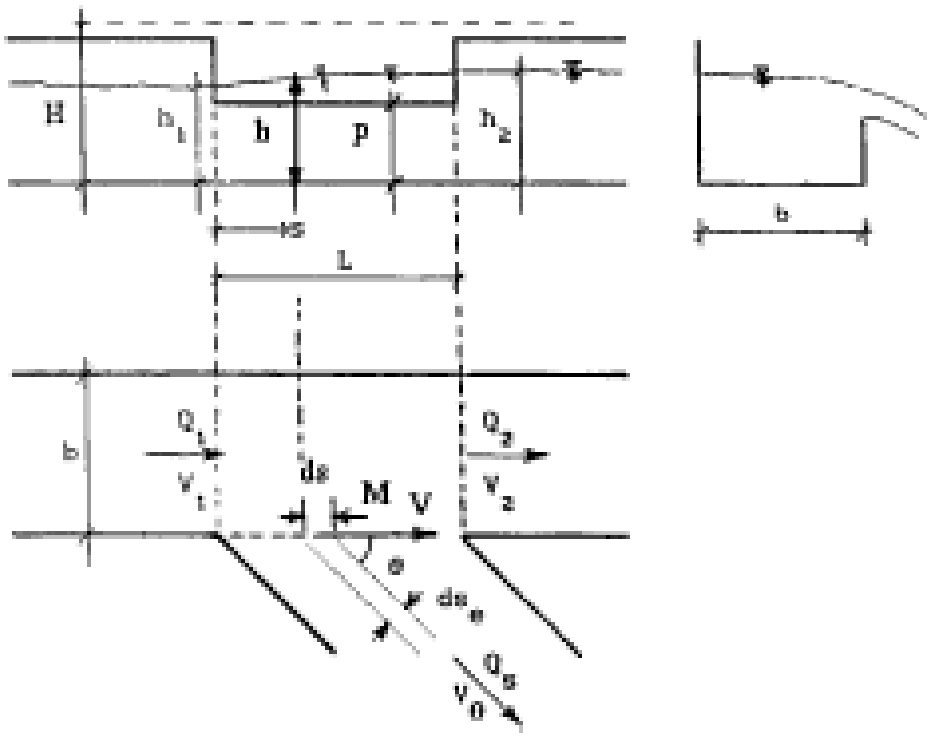

Figure 3.8-1 – Definition Sketch Plan and Elevation

Source: Muslu (2001)

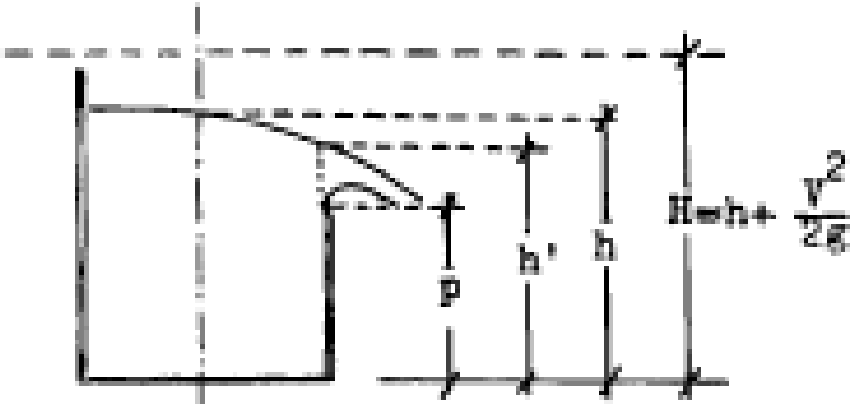

Figure 3.8-2 – Definition Sketch End View

Source: Muslu (2001)

Appendix C

MATLAB CODE

Example Data File Read by Script

File name : 200_0_110

Velocity
Sample,Time,Event Counter,0,,
1,1.500,0,-0.210,-7.280,0.070
2,2.500,0,-0.190,-6.870,-0.370
3,3.500,0,-0.230,-7.660,-0.420
4,4.500,0,-0.110,-7.780,-0.110
5,5.500,0,-0.300,-8.000,-0.200
6,6.500,0,0.430,-7.750,-0.200
7,7.500,0,0.070,-8.380,-0.270
8,8.500,0,0.110,-8.080,0.140
9,9.500,0,0.300,-8.510,-0.390
10,10.500,0,0.160,-7.530,-0.050
11,11.500,0,-0.010,-7.190,-0.150
12,12.500,0,-0.220,-7.890,-0.380
13,13.500,0,0.190,-7.850,-0.270
14,14.500,0,-0.380,-7.920,-0.350
15,15.500,0,-0.210,-6.480,0.440
16,16.500,0,-0.340,-8.190,0.030
17,17.500,0,0.290,-7.310,0.140
18,18.500,0,-0.570,-6.720,-0.510
19,19.500,0,-0.420,-7.170,0.300
20,20.500,0,-0.240,-7.360,-0.380
21,21.500,0,0.000,-9.500,-0.550
22,22.500,0,-0.430,-8.510,-0.410
23,23.500,0,-0.150,-7.330,-0.460
24,24.500,0,-0.260,-7.970,-0.890
25,25.500,0,-0.940,-7.540,-0.080
26,26.500,0,0.290,-7.200,1.020
27,27.500,0,-0.300,-7.990,-1.550
28,28.500,0,0.190,-7.690,-0.080
29,29.500,0,-0.060,-7.580,0.650
30,30.500,0,-0.460,-7.290,-0.540
31,31.500,0,-0.310,-7.520,-0.210
32,32.500,0,0.090,-7.480,-0.020

Matlab Script for Discrete Weir

```
%Velocity Profile

%Written Dave Rowlings 4/10/10

clc
close all
clear all

%Geometric Data
rho=1000;
depth_us=.119;%m
depth_ds=.122;%m
weir_L=.05;%m
width=.300;%m


A_us=depth_us*width;%m^2
A_ds=depth_ds*width;%m^2
R_us=((A_us)/(width+2*depth_us));


q_fm=.140; %m^3/min from flow meter
angle_ave=31-9; % average of discharge angles


%open directory
directory_name = uigetdir('','Select Data Directory');
FileList=dir('*.csv');
N=size(FileList,1);
i=1;


for FileCounter=1:N

    [sample,time,event,x,y,z]=textread(FileList(FileCounter).name,'%f %f %f
%f %f %f',...
        'headerlines',2,'delimiter',',');

    pos=textscan(FileList(FileCounter).name,'%f_%f_%f.vel.csv');

    x_pos(i,:)=pos(1);
    y_pos(i,:)=pos(2);
    z_pos(i,:)=pos(3);

    x_pos_arr=cell2mat(x_pos);%converts from cell format to array
    y_pos_arr=cell2mat(y_pos);
    z_pos_arr=cell2mat(z_pos);

    ave_vx=(sum(x)/length(x));
    ave_vy=abs(sum(y)/length(y));%abs will make the value positive
    ave_vz=(sum(z)/length(z));
```

```
    vx_store(i,:)=ave_vx;
    vy_store(i,:)=ave_vy;
    vz_store(i,:)=ave_vz;

    i=i+1;
end


Z_pos_arr=200-z_pos_arr; %reverses value order so that velocities closest to
the surface are on top

%plot velocity vectors using quiver command, velocities will be 100 times
%larger than they actually are...
figure(1)
hold on
grid on
quiver3(x_pos_arr,y_pos_arr,Z_pos_arr,vx_store,vy_store,vz_store, 0)%plots a
vector profile of the velocities in 3d, 0 prevents scaling
Title('VELOCITY VECTORS');
xlabel('ADV X Position (mm)'); ylabel('ADV Y Position (mm)'); zlabel('ADV Z
Position');
legend('Velocity (scaled up by a factor of 10)')

%place relevant data into single matrix
V=[vx_store, vy_store, vz_store, x_pos_arr, y_pos_arr, Z_pos_arr];

%seperates the velocities into layers
V_top_us=V(1:6:132,:); %#ok<NASGU>
V_mid_us=V(2:6:132,:); %#ok<NASGU>
V_bot_us=V(3:6:132,:); %#ok<NASGU>

V_top_ds=V(4:6:132,:); %#ok<NASGU>
V_mid_ds=V(5:6:132,:); %#ok<NASGU>
V_bot_ds=V(6:6:132,:); %#ok<NASGU>

%converts velocity to m/s
V_top_us_ms=V_top_us(:,1:3)./100;
V_mid_us_ms=V_mid_us(:,1:3)./100;
V_bot_us_ms=V_bot_us(:,1:3)./100;

V_top_ds_ms=V_top_ds(:,1:3)./100;
V_mid_ds_ms=V_mid_ds(:,1:3)./100;
V_bot_ds_ms=V_bot_ds(:,1:3)./100;

%put m/s velocities back into matrix replacing cm/s values
V_top_us=[V_top_us_ms(:,1:3) V_top_us(:,4:6)];
V_mid_us=[V_mid_us_ms(:,1:3) V_mid_us(:,4:6)];
V_bot_us=[V_bot_us_ms(:,1:3) V_bot_us(:,4:6)];

V_top_ds=[V_top_ds_ms(:,1:3) V_top_ds(:,4:6)];
V_mid_ds=[V_mid_ds_ms(:,1:3) V_mid_ds(:,4:6)];
V_bot_ds=[V_bot_ds_ms(:,1:3) V_bot_ds(:,4:6)];
```

```
V_us=[V_top_us;V_mid_us;V_bot_us];
V_ds=[V_top_ds;V_mid_ds;V_bot_ds];

%plot velocity profile contours using contour command
figure(2)
hold on
xx_us=260:2.5:460;
zz_us=min(0):2.5:max(depth_us*1000);%plots contour of entire channel depth
%zz_us=min(V_us(:,6)):max(V_us(:,6));%plots contour of measured section only
[XI_us ZI_us]=meshgrid(xx_us, zz_us);
grid_us=griddata(V_us(:,4),V_us(:,6),V_us(:,2),XI_us, ZI_us, 'V4');
surf(XI_us, ZI_us, grid_us);
title('Upstream Velocity Profile');
xlabel('ADV X position (mm)'); ylabel('ADV Z position (mm)');
zlabel('Velocity (m/s)')

figure(3)
hold on
xx_ds=260:2.5:460;
zz_ds=min(0):2.5:max(depth_ds*1000);%plots contour of entire channel depth
%zz_ds=min(V_ds(:,6)):max(V_ds(:,6));%plots contour of measured section only
[XI_ds ZI_ds]=meshgrid(xx_ds, zz_ds);
grid_ds=griddata(V_ds(:,4),V_ds(:,6),V_ds(:,2),XI_ds, ZI_ds, 'V4');
surf(XI_ds, ZI_ds, grid_ds);
title('Downstream Velocity Profile');
xlabel('ADV X position (mm)'); ylabel('ADV Z position (mm)');
zlabel('Velocity (m/s)')

%calculate mean section velocities
meanV_us=mean(mean(grid_us)); %mean section velocity upstream calculated from
griddata extrapolation
meanV_ds=mean(mean(grid_ds));%mean section velocity down stream calculated
from griddata extrapolation

%%calculate discharges
q_us=meanV_us*A_us;
   %%%mid weir discharge undeterminable as depths not known
q_ds=meanV_ds*A_ds;

%side weir discharge calculated using velocity profiles
q1_sw=q_us-q_ds

%side weir discharge calculated using flow meter and discharge angle
V_fm=(((q_fm/60))/A_us);
V_sw=((V_fm+meanV_ds)/(2*cosd(angle_ave)))
q2_sw=V_sw*(((depth_us+depth_ds)/2)*weir_L)

%%%convert velocities to point momentums
%flow rates
Q_top_us=[(V_top_us(:,1:3).*A_us) V_top_us(:,4:6)];
Q_mid_us=[(V_mid_us(:,1:3).*A_us) V_mid_us(:,4:6)];
Q_bot_us=[(V_bot_us(:,1:3).*A_us) V_bot_us(:,4:6)];

Q_top_ds=[(V_top_ds(:,1:3).*A_us) V_top_ds(:,4:6)];
Q_mid_ds=[(V_mid_ds(:,1:3).*A_us) V_mid_ds(:,4:6)];
```

```
Q_bot_ds=[(V_bot_ds(:,1:3).*A_us) V_bot_ds(:,4:6)];

%momentum
M_top_us=[(V_top_us(:,1:3).*Q_top_us(:,1:3).*rho) V_top_us(:,4:6)];
M_mid_us=[(V_mid_us(:,1:3).*Q_mid_us(:,1:3).*rho) V_mid_us(:,4:6)];
M_bot_us=[(V_bot_us(:,1:3).*Q_bot_us(:,1:3).*rho) V_bot_us(:,4:6)];

M_top_ds=[(V_top_ds(:,1:3).*Q_top_ds(:,1:3).*rho) V_top_ds(:,4:6)];
M_mid_ds=[(V_mid_ds(:,1:3).*Q_mid_ds(:,1:3).*rho) V_mid_ds(:,4:6)];
M_bot_ds=[(V_bot_ds(:,1:3).*Q_bot_ds(:,1:3).*rho) V_bot_ds(:,4:6)];

M_top_loss_y=M_top_us(:,2)-M_top_ds(:,2);
M_mid_loss_y=M_mid_us(:,2)-M_mid_ds(:,2);
M_bot_loss_y=M_bot_us(:,2)-M_bot_ds(:,2);

%average the momentum losses and make an array so it can be plotted
ave_m_top_loss_y=zeros(length(M_top_loss_y),1);
ave_m_top_loss_y(:,1)=sum(M_top_loss_y)/length(M_top_loss_y);

ave_m_mid_loss_y=zeros(length(M_mid_loss_y),1);
ave_m_mid_loss_y(:,1)=sum(M_mid_loss_y)/length(M_mid_loss_y);

ave_m_bot_loss_y=zeros(length(M_bot_loss_y),1);
ave_m_bot_loss_y(:,1)=sum(M_bot_loss_y)/length(M_bot_loss_y);



%%%%%%%%%%%%%%%%%%%%%%%%%%%%%%%%%
%%%longitudinal momentum change%%%
%%%%%%%%%%%%%%%%%%%%%%%%%%%%%%%%%

figure(4)
hold on
grid on
%plot point momentum losses
plot(M_top_us(:,4), M_top_loss_y,'-bs', 'linewidth', 1, ...
                                        'Markeredgecolor', 'k', ...
                                        'Markersize',5, ...
                                        'Markerfacecolor', 'b')
plot(M_mid_us(:,4), M_mid_loss_y,'-yd', 'linewidth', 1, ...
                                        'Markeredgecolor', 'k', ...
                                        'Markersize',5, ...
                                        'Markerfacecolor', 'y')
plot(M_bot_us(:,4), M_bot_loss_y,'-mo', 'linewidth', 1, ...
                                        'Markeredgecolor', 'k', ...
                                        'Markersize',5, ...
                                        'Markerfacecolor', 'm')
%plot average momentum losses
plot(M_top_us(:,4),ave_m_top_loss_y,'--b')

plot(M_mid_us(:,4),ave_m_mid_loss_y,'--y')

plot(M_bot_us(:,4),ave_m_bot_loss_y,'--m')

title('LONGITUDINAL MOMENTUM CHANGE OF MEASURED POINTS ACROSS SIDE WEIR');
```

```
legend('Top Layer Point', 'Mid Layer Point', 'Bottom Layer Point', 'Top Layer
Average Change', 'Mid Layer Average Change', 'Bottom Layer Average Change')
xlabel('ADV X Position (mm)'); ylabel('Momentum Change (N)');
%%%%%%%%%%%%%%%%%%%%%%%%%%%%%%%%
%%%%%%%%%%%%%%%%%%%%%%%%%%%%%%%%
%%%%%%%%%%%%%%%%%%%%%%%%%%%%%%%%



%%%%%%%%%%%%%%%%%%%%%%%%%%%%%%
%%%lateral momentum change%%%
%%%%%%%%%%%%%%%%%%%%%%%%%%%%%%
M_top_loss_x=M_top_us(:,1)-M_top_ds(:,1);
M_mid_loss_x=M_mid_us(:,1)-M_mid_ds(:,1);
M_bot_loss_x=M_bot_us(:,1)-M_bot_ds(:,1);

%average the momentum losses and make an array so it can be plotted
ave_m_top_loss_x=zeros(length(M_top_loss_x),1);
ave_m_top_loss_x(:,1)=sum(M_top_loss_x)/length(M_top_loss_x);

ave_m_mid_loss_x=zeros(length(M_mid_loss_x),1);
ave_m_mid_loss_x(:,1)=sum(M_mid_loss_x)/length(M_mid_loss_x);

ave_m_bot_loss_x=zeros(length(M_bot_loss_x),1);
ave_m_bot_loss_x(:,1)=sum(M_bot_loss_x)/length(M_bot_loss_x);

figure(5)
hold on
grid on
%plot point momentum losses
plot(M_top_us(:,4), M_top_loss_x,'-bs', 'linewidth', 1, ...
                                        'Markeredgecolor', 'k', ...
                                        'Markersize',5, ...
                                        'Markerfacecolor', 'b')
plot(M_mid_us(:,4), M_mid_loss_x,'-yd', 'linewidth', 1, ...
                                        'Markeredgecolor', 'k', ...
                                        'Markersize',5, ...
                                        'Markerfacecolor', 'y')
plot(M_bot_us(:,4), M_bot_loss_x,'-mo', 'linewidth', 1, ...
                                        'Markeredgecolor', 'k', ...
                                        'Markersize',5, ...
                                        'Markerfacecolor', 'm')
%plot average momentum losses
plot(M_top_us(:,4),ave_m_top_loss_x,'--b')

plot(M_mid_us(:,4),ave_m_mid_loss_x,'--y')

plot(M_bot_us(:,4),ave_m_bot_loss_x,'--m')

Title('LATERAL MOMENTUM CHANGE OF MEASURED POINTS ACROSS SIDE WEIR');
Legend('Top Layer Point', 'Mid Layer Point', 'Bottom Layer Point', 'Top Layer
Average Change', 'Mid Layer Average Change', 'Bottom Layer Average Change')
xlabel('ADV X Position (mm)'); ylabel('Momentum Change (N)');
%%%%%%%%%%%%%%%%%%%%%%%%%%%%%%%%
%%%%%%%%%%%%%%%%%%%%%%%%%%%%%%%%
%%%%%%%%%%%%%%%%%%%%%%%%%%%%%%%%
```

```
%%%%%%%%%%%%%%%%%%%%%
%%%flow conditions%%%
%%%%%%%%%%%%%%%%%%%%%
%reynolds number
Re_us=1000*depth_us*V_fm/(4*1.13*10^-3);

%froude number
Fr_us=V_fm/(sqrt(9.81*depth_us))

disp(Re_us);
disp(Fr_us);
```

Matlab Script for Long Weir

```
%Velocity Profile

%Written Dave Rowlings 4/10/10

clc
close all
clear all

%Geometric Data
rho=1000;
depth_us=.118;%m
depth_ds=.1195;%m
width=.300;%m
weir_L=.300;%m

%measured clockwise is positive
us_angle=45;
ds_angle=32;

A_us=depth_us*width;%m^2
A_ds=depth_ds*width;%m^2

q_fm=.195; %m^3/min from flow meter
angle_ave=(us_angle-ds_angle); % average of discharge angles

%open directory
directory_name = uigetdir('','Select Data Directory');
FileList=dir('*.csv');
N=size(FileList,1);
i=1;


for FileCounter=1:N

    [sample,time,event,x,y,z]=textread(FileList(FileCounter).name,'%f %f %f
%f %f %f',...
        'headerlines',2,'delimiter',',');

    pos=textscan(FileList(FileCounter).name,'%f_%f_%f.vel.csv');

    x_pos(i,:)=pos(1);
    y_pos(i,:)=pos(2);
    z_pos(i,:)=pos(3);

    x_pos_arr=cell2mat(x_pos);%converts from cell format to array
    y_pos_arr=cell2mat(y_pos);
    z_pos_arr=cell2mat(z_pos);

    ave_vx=(sum(x)/length(x));
    ave_vy=abs(sum(y)/length(y));%abs will make the value positive
    ave_vz=(sum(z)/length(z));
```

```
    vx_store(i,:)=ave_vx;
    vy_store(i,:)=ave_vy;
    vz_store(i,:)=ave_vz;

    i=i+1;
end


Z_pos_arr=200-z_pos_arr; %reverses value order so that velocities closest to
the surface are on top

%plot velocity vectors using quiver command, velocities will be 100 times
%larger than they actually are...
figure(1)
hold on
grid on
quiver3(x_pos_arr,y_pos_arr,Z_pos_arr,vx_store,vy_store,vz_store, 0)%plots a
vector profile of the velocities in 3d, 0 prevents scaling
title('VELOCITY VECTORS');
xlabel('ADV X Position (mm)'); ylabel('ADV Y Position (mm)'); zlabel('ADV Z
Position');
legend('Velocity (scaled up by a factor of 10)')

%place relevant data into single matrix
V=[vx_store, vy_store, vz_store, x_pos_arr, y_pos_arr, Z_pos_arr];

%seperates the velocities into layers
V_top_us=V(1:9:99,:); %#ok<NASGU>
V_mid_us=V(2:9:99,:); %#ok<NASGU>
V_bot_us=V(3:9:99,:); %#ok<NASGU>

V_top_mw=V(4:9:99,:); %#ok<NASGU>
V_mid_mw=V(5:9:99,:); %#ok<NASGU>
V_bot_mw=V(6:9:99,:); %#ok<NASGU>

V_top_ds=V(7:9:99,:); %#ok<NASGU>
V_mid_ds=V(8:9:99,:); %#ok<NASGU>
V_bot_ds=V(9:9:99,:); %#ok<NASGU>

%converts velocity to m/s
V_top_us_ms=V_top_us(:,1:3)./100;
V_mid_us_ms=V_mid_us(:,1:3)./100;
V_bot_us_ms=V_bot_us(:,1:3)./100;

V_top_mw_ms=V_top_mw(:,1:3)./100;
V_mid_mw_ms=V_mid_mw(:,1:3)./100;
V_bot_mw_ms=V_bot_mw(:,1:3)./100;

V_top_ds_ms=V_top_ds(:,1:3)./100;
V_mid_ds_ms=V_mid_ds(:,1:3)./100;
V_bot_ds_ms=V_bot_ds(:,1:3)./100;

%put m/s velocities back into matrix replacing cm/s values
```

```
V_top_us=[V_top_us_ms(:,1:3) V_top_us(:,4:6)];
V_mid_us=[V_mid_us_ms(:,1:3) V_mid_us(:,4:6)];
V_bot_us=[V_bot_us_ms(:,1:3) V_bot_us(:,4:6)];

V_top_mw=[V_top_mw_ms(:,1:3) V_top_mw(:,4:6)];
V_mid_mw=[V_mid_mw_ms(:,1:3) V_mid_mw(:,4:6)];
V_bot_mw=[V_bot_mw_ms(:,1:3) V_bot_mw(:,4:6)];

V_top_ds=[V_top_ds_ms(:,1:3) V_top_ds(:,4:6)];
V_mid_ds=[V_mid_ds_ms(:,1:3) V_mid_ds(:,4:6)];
V_bot_ds=[V_bot_ds_ms(:,1:3) V_bot_ds(:,4:6)];

V_us=[V_top_us;V_mid_us;V_bot_us];
V_mw=[V_top_mw;V_mid_mw;V_bot_mw];
V_ds=[V_top_ds;V_mid_ds;V_bot_ds];

%plot velocity profile contours using contour command
figure(2)
hold on
xx_us=260:2.5:460;
zz_us=min(0):2.5:max(depth_us*1000);%plots contour of entire channel depth
%zz_us=min(V_us(:,6)):max(V_us(:,6));%plots contour of measured section only
[XI_us ZI_us]=meshgrid(xx_us, zz_us);
grid_us=griddata(V_us(:,4),V_us(:,6),V_us(:,2),XI_us, ZI_us, 'V4');
surf(XI_us, ZI_us, grid_us);
title('Upstream Velocity Profile');
xlabel('ADV X position (mm)'); ylabel('ADV Z position (mm)');
zlabel('Velocity (m/s)')

figure(3)%adjust this one
hold on
xx_mw=260:2.5:460;
zz_mw=min(0):2.5:max(((depth_us+depth_ds)/2)*1000);%plots contour of entire
channel depth
%zz_ds=min(V_ds(:,6)):max(V_ds(:,6));%plots contour of measured section only
[XI_mw ZI_mw]=meshgrid(xx_mw, zz_mw);
grid_mw=griddata(V_mw(:,4),V_mw(:,6), V_mw(:,2),XI_mw, ZI_mw, 'V4');
surf(XI_mw, ZI_mw, grid_mw);
title('Mid Weir Velocity Profile');
xlabel('ADV X position (mm)'); ylabel('ADV Z position (mm)');
zlabel('Velocity (m/s)')

figure(4)
hold on
xx_ds=260:2.5:460;
zz_ds=min(0):2.5:max(depth_ds*1000);%plots contour of entire channel depth
%zz_ds=min(V_ds(:,6)):max(V_ds(:,6));%plots contour of measured section only
[XI_ds ZI_ds]=meshgrid(xx_ds, zz_ds);
grid_ds=griddata(V_ds(:,4),V_ds(:,6),V_ds(:,2),XI_ds, ZI_ds, 'V4');
surf(XI_ds, ZI_ds, grid_ds);
title('Downstream Velocity Profile');
xlabel('ADV X position (mm)'); ylabel('ADV Z position (mm)');
zlabel('Velocity (m/s)')
%calculate mean section velocities
meanV_us=mean(mean(grid_us)) %mean section velocity upstream calculated from
griddata extrapolation
```

```
meanV_mw=mean(mean(grid_mw)) %mean section velocity mid weir calculated from
griddata extrapolation
meanV_ds=mean(mean(grid_ds)) %mean section velocity down stream calculated
from griddata extrapolation

%%calculate discharges
q_us=meanV_us*A_us;
    %mid weir discharge undeterminable as depths not known
q_ds=meanV_ds*A_ds;

%side weir discharge
q_sw=q_us-q_ds

%side weir discharge calculated using flow meter and discharge angle
V_fm=(((q_fm/60))/A_us);
V_sw=(V_fm+meanV_ds)/(2*cosd(angle_ave));
q2_sw=V_sw*(((depth_us+depth_ds)/2)*weir_L)


%%%convert velocities to point momentums
%flow rates
Q_top_us=[(V_top_us(:,1:3).*A_us) V_top_us(:,4:6)];
Q_mid_us=[(V_mid_us(:,1:3).*A_us) V_mid_us(:,4:6)];
Q_bot_us=[(V_bot_us(:,1:3).*A_us) V_bot_us(:,4:6)];

Q_top_ds=[(V_top_ds(:,1:3).*A_us) V_top_ds(:,4:6)];
Q_mid_ds=[(V_mid_ds(:,1:3).*A_us) V_mid_ds(:,4:6)];
Q_bot_ds=[(V_bot_ds(:,1:3).*A_us) V_bot_ds(:,4:6)];

%momentum
M_top_us=[(V_top_us(:,1:3).*Q_top_us(:,1:3).*rho) V_top_us(:,4:6)];
M_mid_us=[(V_mid_us(:,1:3).*Q_mid_us(:,1:3).*rho) V_mid_us(:,4:6)];
M_bot_us=[(V_bot_us(:,1:3).*Q_bot_us(:,1:3).*rho) V_bot_us(:,4:6)];

M_top_ds=[(V_top_ds(:,1:3).*Q_top_ds(:,1:3).*rho) V_top_ds(:,4:6)];
M_mid_ds=[(V_mid_ds(:,1:3).*Q_mid_ds(:,1:3).*rho) V_mid_ds(:,4:6)];
M_bot_ds=[(V_bot_ds(:,1:3).*Q_bot_ds(:,1:3).*rho) V_bot_ds(:,4:6)];

%%%%%%%%%%%%%%%%%%%%%%%%%%%%%%%%%%
%%%longitudinal momentum change%%%
%%%%%%%%%%%%%%%%%%%%%%%%%%%%%%%%%%
M_top_loss_y=M_top_us(:,2)-M_top_ds(:,2);
M_mid_loss_y=M_mid_us(:,2)-M_mid_ds(:,2);
M_bot_loss_y=M_bot_us(:,2)-M_bot_ds(:,2);

%average the momentum losses and make an array so it can be plotted
ave_m_top_loss_y=zeros(length(M_top_loss_y),1);
ave_m_top_loss_y(:,1)=sum(M_top_loss_y)/length(M_top_loss_y);

ave_m_mid_loss_y=zeros(length(M_mid_loss_y),1);
ave_m_mid_loss_y(:,1)=sum(M_mid_loss_y)/length(M_mid_loss_y);

ave_m_bot_loss_y=zeros(length(M_bot_loss_y),1);
ave_m_bot_loss_y(:,1)=sum(M_bot_loss_y)/length(M_bot_loss_y);
```

```
figure(5)
hold on
grid on
%plot point momentum losses
plot(M_top_us(:,4), M_top_loss_y,'-bs', 'linewidth', 1, ...
                                        'Markeredgecolor', 'k', ...
                                        'Markersize',5, ...
                                        'Markerfacecolor', 'b')
plot(M_mid_us(:,4), M_mid_loss_y,'-yd', 'linewidth', 1, ...
                                        'Markeredgecolor', 'k', ...
                                        'Markersize',5, ...
                                        'Markerfacecolor', 'y')
plot(M_bot_us(:,4), M_bot_loss_y,'-mo', 'linewidth', 1, ...
                                        'Markeredgecolor', 'k', ...
                                        'Markersize',5, ...
                                        'Markerfacecolor', 'm')
%plot average momentum losses
plot(M_top_us(:,4),ave_m_top_loss_y,'--b')

plot(M_mid_us(:,4),ave_m_mid_loss_y,'--y')

plot(M_bot_us(:,4),ave_m_bot_loss_y,'--m')

title('LONGITUDINAL MOMENTUM CHANGE OF MEASURED POINTS ACROSS SIDE WEIR');
legend('Top Layer Point', 'Mid Layer Point', 'Bottom Layer Point', 'Top Layer
Average Change', 'Mid Layer Average Change', 'Bottom Layer Average Change')
xlabel('ADV X Position (mm)'); ylabel('Momentum Change (N)');
%%%%%%%%%%%%%%%%%%%%%%%%%%%%%%
%%%%%%%%%%%%%%%%%%%%%%%%%%%%%%
%%%%%%%%%%%%%%%%%%%%%%%%%%%%%%



%%%%%%%%%%%%%%%%%%%%%%%%%%%%%%
%%%lateral momentum change%%%
%%%%%%%%%%%%%%%%%%%%%%%%%%%%%%
M_top_loss_x=M_top_us(:,1)-M_top_ds(:,1);
M_mid_loss_x=M_mid_us(:,1)-M_mid_ds(:,1);
M_bot_loss_x=M_bot_us(:,1)-M_bot_ds(:,1);

%average the momentum losses and make an array so it can be plotted
ave_m_top_loss_x=zeros(length(M_top_loss_x),1);
ave_m_top_loss_x(:,1)=sum(M_top_loss_x)/length(M_top_loss_x);

ave_m_mid_loss_x=zeros(length(M_mid_loss_x),1);
ave_m_mid_loss_x(:,1)=sum(M_mid_loss_x)/length(M_mid_loss_x);

ave_m_bot_loss_x=zeros(length(M_bot_loss_x),1);
ave_m_bot_loss_x(:,1)=sum(M_bot_loss_x)/length(M_bot_loss_x);

figure(6)
hold on
grid on
%plot point momentum losses
plot(M_top_us(:,4), M_top_loss_x,'-bs', 'linewidth', 1, ...
```

```
                                        'Markeredgecolor', 'k', ...
                                        'Markersize',5, ...
                                        'Markerfacecolor', 'b')
plot(M_mid_us(:,4), M_mid_loss_x,'-yd', 'linewidth', 1, ...
                                        'Markeredgecolor', 'k', ...
                                        'Markersize',5, ...
                                        'Markerfacecolor', 'y')
plot(M_bot_us(:,4), M_bot_loss_x,'-mo', 'linewidth', 1, ...
                                        'Markeredgecolor', 'k', ...
                                        'Markersize',5, ...
                                        'Markerfacecolor', 'm')
%plot average momentum losses
plot(M_top_us(:,4),ave_m_top_loss_x,'--b')

plot(M_mid_us(:,4),ave_m_mid_loss_x,'--y')

plot(M_bot_us(:,4),ave_m_bot_loss_x,'--m')

title('LATERAL MOMENTUM CHANGE OF MEASURED POINTS ACROSS SIDE WEIR');
legend('Top Layer Point', 'Mid Layer Point', 'Bottom Layer Point', 'Top Layer
Average Change', 'Mid Layer Average Change', 'Bottom Layer Average Change')
xlabel('ADV X Position (mm)'); ylabel('Momentum Change (N)');
%%%%%%%%%%%%%%%%%%%%%%%%%%%%%%
%%%%%%%%%%%%%%%%%%%%%%%%%%%%%%
%%%%%%%%%%%%%%%%%%%%%%%%%%%%%%



%%%%%%%%%%%%%%%%%%%%%%
%%%flow conditions%%%
%%%%%%%%%%%%%%%%%%%%%%
%reynolds number
Re_us=1000*depth_us*V_fm/(4*1.13*10^-3)

%froude number
Fr_us=V_fm/(sqrt(9.81*depth_us))
```

Appendix D

LATERAL FLOW MODEL

Lateral Flow Model

Lateral Weir Flow Model

assumptions	**1. Flow upstream is subcritical**		
	2. Length of weir is limited to the width of the channel		

Discrete

	knowns		
L	0.05	*m*	*length of weir, cannot exceed B*
B	0.3	*m*	*width of channel*
L/B	0.166667		*geometric ratio*
V_1	0.065	*m/s*	*velocity upstream*
S	0.1	*m*	*the height of the weir from the channel base*
y_1	0.119	*m*	*height of water upstream*
h_0	0.019	*m*	*height of water at the upstream end of the weir*
F_1	0.06053		*froude number upstream, should be less than 1 (ie subcritical flow)*
F_0	0.151484		*froude number over weir*
η_0	0.106506		*velocity ratio*
V_{j_barr}	0.413563	*m/s*	*mean velocity over weir*

Taylor Series Approximations used to find Cd

c_1	-0.49833		
c_2	0.097		
c_3	-0.21167		
$f(\eta_0,L/B)$	163.6575		*function of velocity and geometric ratios*
C_{d_barr}	0.593888		*mean coefficient of discharge for side weir*
Q_t	0.000233	m^3/s	*discharge over weir*
Q_1	0.002335	m^3/s	*discharge upstream*
Q_2	0.002101	m^3/s	*discharge downstream*

Long

L	0.3	*m*	*length of weir, cannot exceed B*
B	0.3	*m*	*width of channel*
L/B	1		*geometric ratio*
V_1	0.092	*m/s*	*velocity upstream*
S	0.1	*m*	*the height of the weir from the channel base*
y_1	0.118	*m*	*height of water upstream*
h_0	0.018	*m*	*height of water at the upstream end of the weir*
F_1	0.085323		*froude number upstream, should be less than 1 (ie subcritical flow)*
F_0	0.21846		*froude number over weir*
η_0	0.152664		*velocity ratio*
V_{j_barr}	0.408986	*m/s*	*mean velocity over weir*

Taylor Series Approximations used to find Cd

c_1	-0.29		
c_2	0.292		
c_3	-0.62		
$f(\eta_0,L/B)$	55.28309		*function of velocity and geometric ratios*
C_{d_barr}	0.592202		*mean coefficient of discharge for side weir*
Q_t	0.001308	m^3/s	*discharge over weir*
Q_1	0.00325	m^3/s	*discharge upstream*
Q_2	0.001942	m^3/s	*discharge downstream*

Appendix E

LATERAL INFLOW/OUTFLOW CALCULATIONS

Long weir Lateral Inflow

	x_i	y_i	y_{bar}	A_{bar}	P_{bar}	S_f	ΔQ	Q_i	Q_{bar}	dy/dx
300	0	0.1195						0.0006		
			0.119	0.036	0.53897	0.00000097	0.000281		0.000726	-3.19221E-05
250	-0.05	0.1195						0.0009		
			0.119	0.036	0.5389	0.00000187	0.000280		0.001006	-4.44128E-05
200	-0.1	0.1194						0.0011		
			0.119	0.036	0.5388	0.00000306	0.000279		0.001286	-5.67864E-05
150	-0.15	0.1194						0.0014		
			0.119	0.036	0.53867	0.00000454	0.000278		0.001565	-6.89986E-05
100	-0.2	0.1193						0.0017		
			0.119	0.036	0.53852	0.00000630	0.000276		0.001842	-8.10326E-05
50	-0.25	0.1192						0.0020		
			0.119	0.036	0.53835	0.00000834	0.000274		0.002117	-9.28604E-05
0	-0.3	0.11913						0.0023		
					Weir Discharge		**0.001669**			

Long Weir Lateral Outflow

x_i	y_i	y_{bar}	A_{bar}	P_{bar}	S_f	ΔQ	Q_i	Q_{bar}	dy/dx
0	0.11950						0.0006		
		0.119	0.036	0.53895	0.00000	0.000281		0.000725	-1.57231E-05
-0.05	0.11945						0.0009		
		0.119	0.036	0.53884	0.00000	0.000280		0.001006	-2.19504E-05
-0.1	0.11939						0.0011		
		0.119	0.036	0.53872	0.00000	0.000278		0.001285	-2.81215E-05
-0.15	0.11933						0.0014		
		0.119	0.036	0.53859	0.00000	0.000277		0.001563	-3.42302E-05
-0.2	0.11926						0.0017		
		0.119	0.036	0.53844	0.00001	0.000275		0.001839	-4.0257E-05
-0.25	0.11918						0.0020		
		0.119	0.036	0.53828	0.00001	0.000274		0.002113	-4.62034E-05
-0.3	0.11910						0.0023		
				Weir Discharge		**0.001665**			

Discrete Weir Lateral Inflow

	x_i	y_i	y_{bar}	A_{bar}	P_{bar}	S_f	ΔQ	Q_i	Q_{bar}	dy/dx
50	0	0.1220						0.0021		
			0.122	0.037	0.544	0.00001	0.000067		0.002134	-2.1946E-05
40	-0.01	0.1220						0.0022		
			0.122	0.037	0.5438	0.00001	0.000067		0.002201	-0.00022544
30	-0.02	0.1218						0.0022		
			0.122	0.037	0.5434	0.00001	0.000066		0.002267	-0.000229887
20	-0.03	0.1216						0.0023		
			0.122	0.036	0.543	0.00001	0.000065		0.002333	-0.0002341
10	-0.04	0.1214						0.0024		
			0.121	0.036	0.5426	0.00001	0.000064		0.002398	-0.000238083
0	-0.05	0.1212						0.0024		
					Weir Discharge		**0.000330**			

Discrete Weir Lateral Outflow

x_i	y_i	y_{bar}	A_{bar}	P_{bar}	S_f	ΔQ	Q_i	Q_{bar}	dy/dx
0	0.12200						0.0021		
		0.122	0.037	0.54399	0.00001	0.000067		0.002134	-1.09598E-05
-0.01	0.12199						0.0022		
		0.122	0.037	0.54397	0.00001	0.000067		0.002201	-1.13081E-05
-0.02	0.12198						0.0022		
		0.122	0.037	0.54395	0.00001	0.000067		0.002268	-1.1656E-05
-0.03	0.12197						0.0023		
		0.122	0.037	0.54393	0.00001	0.000067		0.002336	-1.20038E-05
-0.04	0.12196						0.0024		
		0.122	0.037	0.54391	0.00001	0.000067		0.002403	-1.23513E-05
-0.05	0.12195						0.0024		
				Weir Discharge		**0.000337**			